PHYSICAL REVIEW
LETTERS

VOLUME 7 NOVEMBER 15, 1961 NUMBER 10

SPECIFIC HEAT OF SOLID He^3†

E. C. Heltemes and C. A. Swenson
Institute for Atomic Research and Department of Physics, Iowa State University, Ames, Iowa
(Received October 23, 1961)

Various measurements have been reported on physical properties of solidified He^3,[1-4] with no correlation between many of them. A large exchange interaction between the nuclear spins in the solid has been predicted by Bernardes and Primakoff,[5] and a reduction of the entropy due to this ordering should be apparent as a specific heat anomaly. The pressure dependence of this exchange interaction is not known, and the initial purpose of the present experiments was to attempt to ascertain whether or not it became large at high pressures. Solid He^3 is of interest also because it exists in a bcc phase (αHe^3) at relatively low pressures.[6] This phase is anomalous in that theoretical calculations have suggested that it should not be stable at any pressure with respect to the normal hcp phase (βHe^3).[7]

The measurements were made using a technique which has been described elsewhere.[8] The temperature range (0.3 to 2°K) was determined at the lower limit by the use of a magnetic refrigerator and at the upper limit by heat leak through the lead valve which connected the calorimeter to the heat reservoir. Amounts of He^3 of up to 0.07 mole were compressed into a beryllium copper calorimeter (0.779 cm^3 volume) using pressures as great as 1800 bars at temperatures near the melting line. The temperatures were measured with an "Old Speer" $\frac{1}{2}$-w resistor which was calibrated against a sphere of potassium chrome alum. The calorimeter was kept at liquid nitrogen temperature or below for two months during the course of these measurements, and the calibration of the resistor remained stable during this time. The actual quantity of He^3 in the calorimeter was not measured directly, but rather, the temperature of the calorimeter was monitored upon cooling at constant volume, and the temperatures at which freezing began, T_M, and was completed, T_F, were noted. Liquid hydrogen was used in the Dewar prior to using liquid helium to obtain some of the smaller molar volumes. Previous data[6,9] for the molar volumes of the liquid and the solid along the melting line were then used to calculate the appropriate molar volumes for each of these temperatures for each run. In all cases, the molar volumes as calculated from T_M and T_F were consistent to 0.1 cm^3/mole. It is believed that this represents the uncertainty in our molar volumes, and gives some assurance that the pressures were uniform.

The heat capacity of the empty calorimeter and addenda was measured at three separate times, and was found to be linear in temperature from 0.3 to 1.1°K with a coefficient of $0.30(\pm 0.01)\times 10^{-3}$ cal/deg^2 for the 45-g calorimeter. This linear behavior gives confidence in the temperature scale in this temperature region. A rapid rise in the calorimeter heat capacity above 1.1°K was attributed to heat leak through the lead valve. Thus, there is a basic uncertainty in our data between 1.1 and 2°K due to this factor.

Data were obtained for He^3 for 7M volumes in the α phase and for 10M volumes in the β phase. The techniques which were used were checked through a measurement of the specific heat of solidified He^4 at 12 different molar volumes, which could be compared with previous work.[10] A plot of C/T vs

T^2, as corrected for the calorimeter, indicated a low-temperature anomaly for both He^3 and He^4 of about 15 to 20% of the empty calorimeter value which appeared as a finite extrapolated value of C/T at $T=0$. This appeared in runs where the other specific heat contributions were small, and its cause is not known. The values of the Debye θ which are given in Fig. 1 were determined from these plots by ignoring this contribution, since a comparison of our He^4 data with those of Dugdale and Simon[10] (also shown in Fig. 1, where $\theta/2$ has been plotted for He^4 to separate the curves) showed good agreement using this pragmatic approach. Thus, we must postulate a low-temperature anomaly (whose extent varies somewhat with molar volume) which occurs either in our calorimeter when it contains a sample, or in both He^3 and He^4. This effect must be investigated further, with larger ratios of sample to empty calorimeter specific heats. The inclusion of an additional linear term to the heat capacities will not change the general features of Fig. 1.

The Grüneisen constant $\gamma = -d\ln\theta/d\ln V$ is the same for both phases of He^3 and He^4 within experimental accuracy. The difference between our θ values and those of Dugdale and Simon may be due partially to the fact that their data, which were obtained at higher temperatures, did not obey a Debye relationship, and a comparison could be made only by extrapolating their data to very low temperatures. The falling off of the higher θ's for βHe^3 is probably an experimental effect due to lack of precision in our data. Both He^4 and βHe^3 have the same (hcp) structure in this temperature and pressure region, so a direct comparison can be made of their Debye θ's. The observed ratio of $\theta_3/\theta_4 = 1.19$ is quite close to the value $(\frac{4}{3})^{0.5} = 1.16$ which the elementary theory would predict. Bernardes has calculated θ values for both He^4 and βHe^3 which are about 10% higher than we observe.[7]

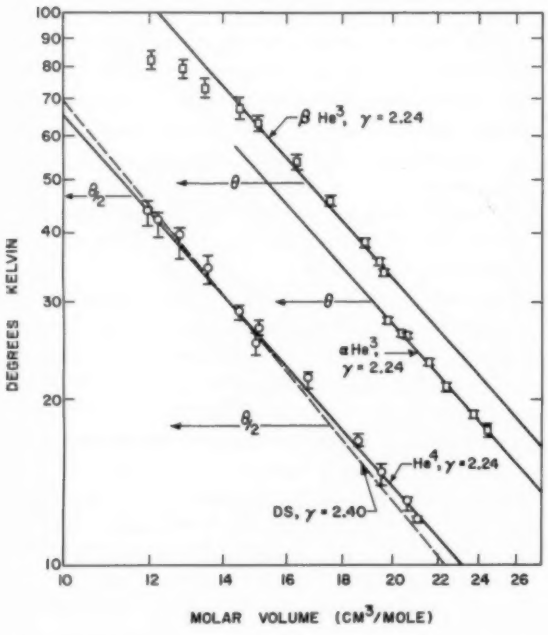

FIG. 1. The volume dependence of the Debye θ for both phases of He^3 and He^4. $\theta/2$ is plotted for He^4 for clarity. The dashed line represents an extrapolation of the data of reference 10 to low temperatures.

The α-β phase transition is seen easily in Fig. 1, where a difference in θ of about 6°K (roughly 20%) is indicated for the two phases. The phase transition was not observed directly in the specific heat measurements because of the small volume difference between the phases. The θ's of He^4 and αHe^3 are almost identical, which is probably fortuitous.

The most interesting feature of these measurements occurs in the αHe^3 phase. A positive and very large deviation from a T^3 specific heat dependence is found for this phase with increasing temperature, and exists up to the melting line for at least the larger molar volumes. This deviation is a function of volume, and can be expressed in terms of a characteristic temperature $\phi(V)$. C/R is given as a function of T/ϕ in Fig. 2, where the apparently linear dependence of ϕ on volume also is shown. The solid curve gives the Einstein specific heat for a system with a characteristic temperature ϕ and two degrees of freedom, which would be typical of an excitation from a ground state to a doubly-degenerate excited state. The data do not extend to sufficiently high values of T/ϕ to detect the existence of higher excited states, if any exist.

There is little evidence of this effect in previous data. The anomalies in the nuclear susceptibility occur at much lower temperatures,[2] and might be associated with our low-temperature "anomaly." Thermal conductivity measurements[1] show unusual behavior in the αHe^3 phase above roughly 1°K, but the relationship of these data with the present measurements is not obvious. Because of the lack of evidence from the nuclear susceptibility measurements, this Einstein-type contribution to the specific heat most likely is associated with the bcc structure of the α phase. This structure should not be stable with respect to the close-packed

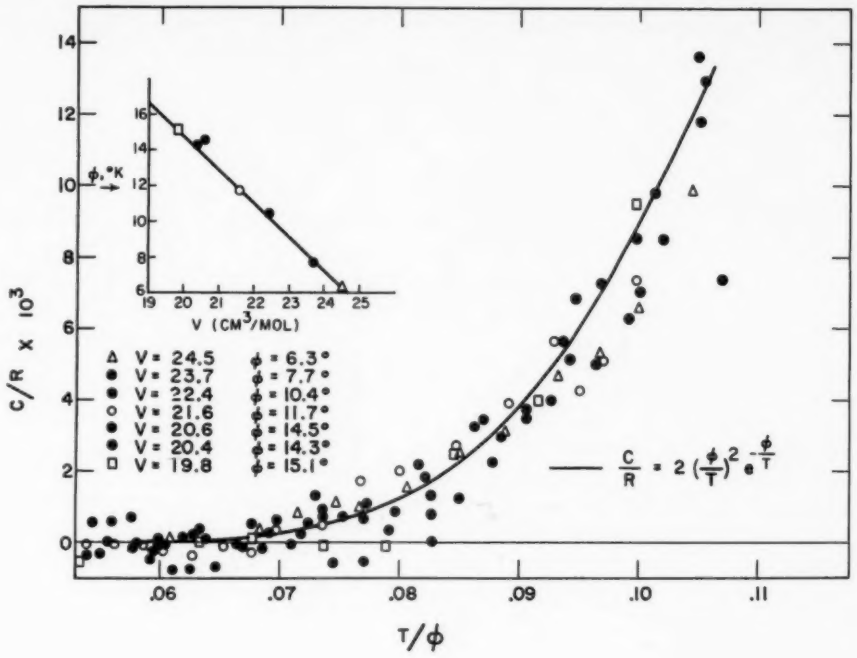

FIG. 2. The anomalous contribution to the specific heat of αHe^3. The heat capacity of the calorimeter and a Debye contribution have been subtracted from the experimental data to obtain this plot. The insert gives the dependence of the characteristic temperature ϕ on volume, and the solid curve shows the theoretical Einstein (or Schottky) specific heat for a system with an energy difference $k\phi$ between the ground state and a doubly-degenerate excited state.

structures,[7] and its very existence is probably indicative of unusual properties of this solid. There is a suspicion that the third phase of He^4 is also bcc,[11] and measurements on this phase would be interesting, but also very difficult due to its location and limited extent on the phase diagram.

A more complete discussion of this work will appear elsewhere. The authors are indebted to H. H. Sample who took and analyzed the He^4 data, and to R. Phillips and M. Yetley who assisted in the analysis of all of the data. Appreciation also is expressed to Dr. N. Bernardes for many stimulating discussions on this problem.

---

†Contribution No. 1080. This work was performed in the Ames Laboratory of the U. S. Atomic Energy Commission.

[1]E. J. Walker and H. A. Fairbank, Phys. Rev. Letters 5, 139 (1960).

[2]E. D. Adams, H. Meyer, and W. M. Fairbank, Helium Three, edited by J. G. Daunt (Ohio State University Press, Columbus, Ohio, 1960), p. 57.

[3]J. M. Goodkind and W. M. Fairbank, Phys. Rev. Letters 4, 458 (1960).

[4]E. R. Grilly and E. F. Hammel, Progress in Low-Temperature Physics, edited by C. J. Gorter (North-Holland Publishing Company, Amsterdam, 1961), Vol. III, p. 196.

[5]N. Bernardes and H. Primakoff, Phys. Rev. 119, 968 (1960).

[6]E. R. Grilly and R. L. Mills, Ann. Phys. 8, 1 (1959).

[7]N. Bernardes, Phys. Rev. 120, 1927 (1960).

[8]E. C. Heltemes and C. A. Swenson, J. Chem. Phys. (to be published).

[9]R. L. Mills, E. R. Grilly, and S. G. Sydoriak, Ann. Phys. 12, 41 (1961).

[10]J. S. Dugdale and F. E. Simon, Proc. Roy. Soc. (London) A218, 291 (1953).

[11]N. Bernardes (to be published).

MAGNETIC PROPERTIES OF He^3 AT PRESSURES NEAR THE MINIMUM IN THE MELTING CURVE*

A. C. Anderson, W. Reese,† and J. C. Wheatley‡
Department of Physics, University of Illinois, Urbana, Illinois
(Received October 13, 1961; revised manuscript received October 30, 1961)

Recent measurements of the specific heat[1] and the velocity of sound[2] of He^3 at pressures slightly above the minimum of the melting curve, P_{min}, and temperatures below 0.1°K have shown departures from the behavior of both the liquid at pressures less than P_{min} and the solid. The purpose of this Letter is to report measurements of magnetic properties of He^3 in this region of the phase diagram which also indicate anomalous behavior.

In these measurements the self-diffusion coefficient, D, the transverse relaxation time, T_2, and the magnetic susceptibility, χ, were measured by the use of the method of spin echoes using the apparatus and techniques described elsewhere.[3,4] The longitudinal relaxation time, T_1, was estimated by observing the time necessary for the magnetization to recover after having been destroyed. The thermometer used was the same magnetic thermometer described in reference 3, and was calibrated by measuring the self-diffusion coefficient at temperatures less than 0.1°K and a pressure of 13 cm Hg and comparing with the results of reference 3.

When working at pressures greater than P_{min}, a plug of solid He^3 was formed in the tube through which the pressure was applied to the sample so that the pressures quoted refer to the pressures at which the plug formed and not necessarily to those of the sample at the temperatures at which the measurements were being made. Although the exact region of the phase diagram in which these measurements were carried out is not known with certainty, it is probable that the present measurements were made in the same region of the phase diagram as the measurements of specific heat and velocity of sound since a similar technique was employed in each case.

The principal results of these measurements are as follows. At a pressure of 28.9 atm, below P_{min}, the liquid behaved in a manner similar to that of the liquid at lower pressures; the diffusion coefficient increasing with decreasing temperature, being 2.6×10^{-4} cm²/sec at 0.033°K, T_2 being greater than 0.75 sec, T_1 being of the order of 10 sec, and the susceptibility being nearly constant with temperature. At 29.5 atm, a pressure slightly greater than P_{min}, this behavior changed greatly. The diffusion coefficient became too small to be

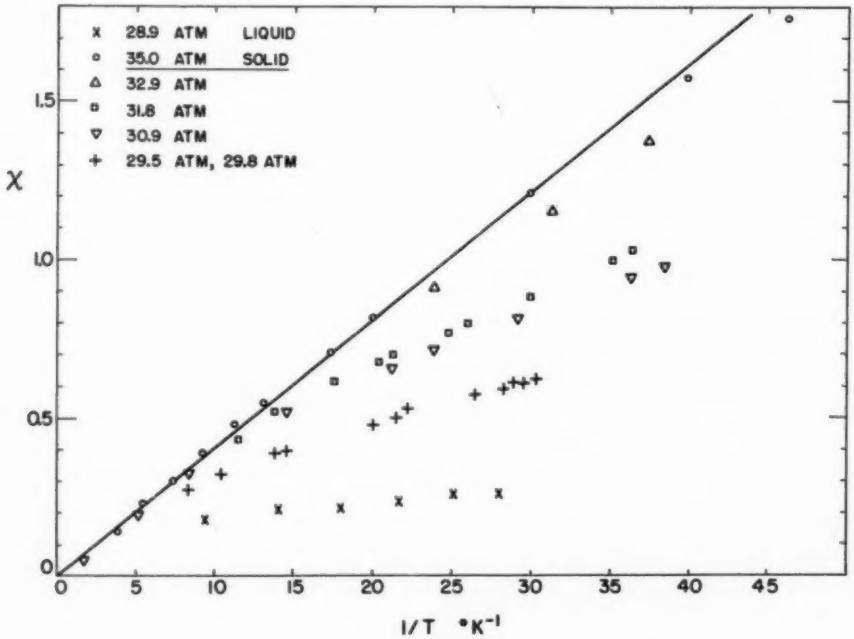

FIG. 1. Susceptibility of He^3, χ, in arbitrary units vs $1/T$. The points are averages of the raw data at each temperature. The solid line represents the best Curie law fit to the 35.0-atm solid data. The pressures for all but the 28.9-atm liquid data are the pressures at which the plug of solid He^3 was initially formed. The data for 29.5 atm and 29.8 atm are shown with the same symbol since no difference could be distinguished between them. Quite possibly this is the result of irreproducibility in the process of forming the plug.

measured with the present apparatus, being less than 5×10^{-7} cm^2/sec, while T_2 decreased to 0.34 $\pm$0.02 sec and T_1 decreased to be of the same order as T_2. At 0.033°K the susceptibility was a factor of 2 larger at 29.5 atm than at 28.9 atm and displayed a considerably different temperature dependence at the higher pressures from that of the liquid below P_{min}. No difference in T_2, T_1, or D could be observed either upon further increasing the pressure or by heating the He^3 to temperatures where the solid phase should exist.

A portion of the susceptibility data is shown in Fig. 1. It should be noted that in addition to the change in behavior of the susceptibility between 28.9 and 29.5 atm, the susceptibility obeyed Curie's law much better at pressures of 32.9 atm and above than at lower pressures. It is interesting to note that in the region between 29.5 atm and 31.8 atm the susceptibility seems to break away from Curie's law near the temperatures where the melting curve of Edwards et al.[5] would predict the solid-liquid phase boundary to occur if the pressure of the sample were that at which the plug was formed.

In view of the measurements of specific heat, sound velocity, susceptibility, T_1, T_2, and D, it appears that the nature of He^3 in the region of the phase diagram of pressures greater than P_{min} and temperature less than about 0.1°K is not understood. It is possible that a new phase of solid, rather than liquid, exists in this region, although further experimentation will be necessary to establish such a fact.

We wish to thank Mr. W. R. Abel, Mr. M. Kuchnir, and Dr. G. L. Salinger for help in making the measurements.

---

*This work has been supported by the U. S. Atomic Energy Commission and the Alfred P. Sloan Foundation.

†National Science Foundation Pre-doctoral Fellow.

‡A. P. Sloan Fellow.

[1]A. C. Anderson, G. L. Salinger, W. A. Steyert, and J. C. Wheatley, Phys. Rev. Letters 7, 295 (1961).

[2]W. R. Abel, A. C. Anderson, and J. C. Wheatley, Phys. Rev. Letters 7, 299 (1961).

[3]A. C. Anderson, W. Reese, R. J. Sarwinski, and J. C. Wheatley, Phys. Rev. Letters 7, 220 (1961).

[4]A. C. Anderson, W. Reese, and J. C. Wheatley (to be published).

[5]D. O. Edwards, J. L. Baum, D. F. Brewer, J. G. Daunt, and A. S. McWilliams, in Helium Three, edited by J. G. Daunt (Ohio State University Press, Columbus, Ohio, 1960). p. 126.

BEHAVIOR OF STRONGLY SHOCKED CARBON*

B. J. Alder and R. H. Christian†

Lawrence Radiation Laboratory, University of California, Livermore, California

(Received October 13, 1961)

This Letter gives evidence for the conversion of graphite to the diamond phase when it is subjected to strong, explosively generated shocks. Furthermore, the data lend support to a further conversion at still higher pressures to a new, higher density phase of carbon, presumably the close-packed metallic liquid.

The initial material was, in the majority of the experiments, natural graphite from Ceylon of very high purity which was pressed into suitable uniform-density pellets of about 95% of theoretical density. Some work was done with commercial graphite, which has a density of 75% of theoretical.

The samples were mounted on an aluminum plate, and by optical means[1] both the shock and free surface velocity of carbon and aluminum were determined. The measurements on the aluminum standard could then be used to determine the pressure-volume point of carbon from its measured shock velocity. This is a more reliable procedure than the use of the free surface velocity when the material does not have a simple behavior. The data are presented in Fig. 1, where the specific volume has been used to avoid artificial corrections due to varying initial densities. However, a correction to the pressure or volume still needs to be made for the increased energy content resulting from a greater change in volume of an initially low-density sample. This correction is insignificant except for samples of $\frac{3}{4}$ theoretical density.

The shock data at low pressures agree with the x-ray determination of crystal densities under pressure[2] as shown by the triangles in Fig. 1. At somewhat higher pressures the static data of Bridgman[3] are indicated by squares in Fig. 1. Again the agreement is good if those data are corrected for the alleged error in the pressure

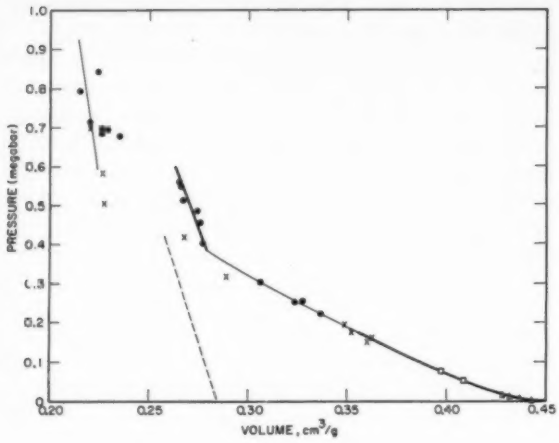

FIG. 1. The Hugoniot equation of state of graphite. Δ—x-ray determination of crystal densities under pressure[2]; □—static data of Bridgman[3]; ×—results for sample of low initial density; ●—results for samples with initially higher density; dashed line—extrapolated static compressibility curve of diamond.

scale.[4] Furthermore, there are eight additional shock experiments available below 0.3 megabar,[5] which are not shown on the graph. These unpublished data are in excellent agreement with the present work.

The Hugoniot below about 0.18 megabar is well behaved in that the rarefaction velocity, calculated as the difference between the measured free surface velocity of the carbon sample and the particle velocity obtained from the matching conditions at the aluminum-carbon interface, indicates that the graphite sample rarefies to the theoretical density of graphite. Above that pressure, however, the free surface velocity is such that the final density is greater than that of crystalline graphite. Furthermore, in the region between 0.18 megabar and 0.4 megabar the free surface velocity is dependent on the thickness of the sample. This phenomenon is a characteristic of a relaxation process of duration comparable to shock transit times. The interpretation of the free surface data is thus consistent with partial conversion of graphite to diamond; the larger graphite samples have more time to convert and the rarefaction leads to a density intermediate between graphite and diamond. The thickness variation of the free surface velocity in the 0.3-megabar experiments is such that an infinitely thin sample would rarefy to crystalline graphite and a $\frac{1}{4}$-inch sample is about 40% converted. The curve between 0.18 and 0.4 megabar has thus been drawn lightly to indicate that the Hugoniot obtained might depend on the initial conditions such as density, temperature, and thickness of sample. It can be noted that the low-initial-density sample (indicated by crosses) at slightly above 0.3 megabar has a higher final density consistent with a higher fraction of conversion because of a larger energy content (temperature) than the samples with initially higher density (indicated by circles), although the uncertainties in the measurements from low-density samples are larger. At 0.2 megabar where the fraction converted is small, the low- and high-density samples give the same results.

The temperature at 0.18 megabar can be estimated as only 500°K by taking account of adiabatic and of irreversible heating. The temperature estimates given here are very rough due to uncertainties in the thermodynamic data[6] and temperature-dependent heat capacities. Although static data indicate that under these conditions diamond is the stable phase,[7] the reaction time would be expected to be extremely long if indeed it were at all possible to affect the direct conversion by the mechanisms considered statically.[8] As with other transitions observed under shock, particularly in the various forms of phosphorus,[9] the rapidity of reaction under shock seems to be connected with the extremely large shear forces in the shock front. When the pressure is released, on the other hand, by an adiabatic rarefaction, the temperatures are so low that a reconversion is not expected from statically determined reaction rates. It is thus not surprising that recovery of shocked graphite has shown diamond to be present.[10-12]

A definite break in the Hugoniot curve can be observed at 0.4 megabar when the graphite has been shocked to a density exceeding that of pure diamond under normal conditions. The presumption then is that conditions have been achieved where the reaction rate is such that less than a microsecond is required for nearly complete conversion to diamond. The slope and position of the curve between 0.4 and 0.6 megabar supports this view since it is in reasonable agreement with the extrapolated static compressibility curve of diamond (dashed line). The static curve actually lies at about 5% higher densities, but this could be due to many causes such as corrections for change of compressibility with pressure, uncertainties in the static compressibility[13] itself, temperature corrections, and incomplete con-

version; all of these tend to give corrections in the proper direction. The temperature at 0.4 megabar is estimated to be 800°K if to the previously mentioned energy contributions the further uncertain heat of conversion is added as obtained by a large extrapolation of static data.[6] The temperature at 0.6 megabar is then estimated to be 1300°K. It is unfortunate that due to the high shock velocity in diamond the free surface velocity measurements in the geometry utilized were not interpretable so that it is not possible to determine the density upon rarefaction, but it is expected to be diamond densities.

At 0.6 megabar the shock velocity in the graphite becomes insensitive to pressure. This is characteristic of the two-shock structure associated with a phase change in which only the leading shock is recorded. The data at yet higher pressure give an indication of the Hugoniot of the new phase. The data show a relatively large scatter since the pressure is near the upper limit of the presently used technique; hence the line is drawn lightly. The data points at 0.7 megabar scatter since they are still in the double shock region.

The volume change (15%) associated with the transition is quite large. It is similar to the transition which has been observed in isomorphous germanium both statically[14] and dynamically.[15] Dynamically it was found that the volume change is comparable, and statically that it was associated with the breakdown of the loosely packed diamond lattice into a metallic, close-packed liquid. Since the volume change is comparable in germanium and carbon and since the entropy change upon melting involving similar structural changes can also be expected to be com parable, it is possible to use the experimental melting temperature dependence with pressure for germanium (corrected for the change in static pressure scale) to determine the melting point for diamond at low pressures—namely about 4000°K. This is in agreement with static expectations. Again the initially low-density samples should transform at lower pressures as the data confirm. The two crossed points in the 0.5- to 0.6-megabar region lie approximately on the extension of the top section of the Hugoniot. These low-density points are, however, approximate as the cross slightly above 0.4 megabar indicates, since in that region the results should not strongly depend on temperature.

---

*This work was performed under the auspices of the U. S. Atomic Energy Commission.

†Also at General Electric Company, Santa Barbara, California.

[1]R. G. McQueen and S. P. Marsh, J. Appl. Phys. 31, 1253 (1960).

[2]L. F. Vereshchagin, Progress in Very High Pressure Research (John Wiley & Sons, Inc., New York, 1961), p. 290.

[3]P. W. Bridgman, Proc. Am. Acad. Arts and Sci. 76, 55 (1948).

[4]G. C. Kennedy and P. N. LaMori, Progress in Very High Pressure Research (John Wiley & Sons, Inc., New York, 1961), p. 304.

[5]J. M. Walsh (private communciation, 1956).

[6]R. Berman and F. Simon, Z. Elektrochem. 59, 333 (1955).

[7]F. P. Bundy, H. P. Bovenkerk, H. M. Strong, and R. H. Wentdorf, J. Chem. Phys. 35, 383 (1961).

[8]H. T. Hall, Proceedings of Symposium on High Temperature (Stanford Research Institute, Stanford, California, 1956), p. 161.

[9]R. Grover, R. H. Christian, and B. J. Alder, Bull. Am. Phys. Soc. 3, 230 (1958).

[10]P. S. DeCarli and J. C. Jamieson, Science 133, 1821 (1961).

[11]C. A. Parsons, Phil. Trans. Roy. Soc. (London) A220, 67 (1918).

[12]"Chementator," Chem. Eng. 66, 71 (1959).

[13]H. J. McSkimin and W. L. Bond, Phys. Rev. 105, 116 (1957).

[14]H. T. Hall, J. Phys. Chem. 59, 1144 (1955).

[15]Unpublished work.

MAGNETORESISTANCE OF TRANSITION METALS IN THE HIGH-FIELD LIMIT

E. Fawcett*
Physics Department, Royal Radar Establishment, Malvern, England
(Received October 16, 1961)

Information about the electronic structure of a metal may be obtained from a study of its magnetoresistance in the high-field limit, in which $\omega_c\bar{\tau} \gg 1$ for all cyclotron orbits on all sheets of the Fermi surface, ω_c being the cyclotron frequency and $\bar{\tau}$ the relaxation time averaged over the orbit. In odd-valent metals the resistivity tends to saturation as the high-field limit is approached, except for field directions such that open orbits on a multiply-connected sheet of the Fermi surface contribute to the conductivity, in which case the resistivity approaches quadratic variation with the magnetic field. In even-valent metals the cancellation of the linear Hall term in the conductivity tensor due to the equal numbers of electrons and holes leads to quadratic variation for general field and current orientations. This remains true for multiply-connected surfaces, but open orbits nearly perpendicular to the current direction will now lead to saturation for the corresponding field direction.[1]

The extension of these ideas to the transition metals is by no means obvious, if only for the simple reason that the chemical valency will not in general equal the number of conduction electrons, i.e., the number of occupied states in partially filled Brillouin zones. However, it is proposed here that this number is always odd or even as the atomic number[2] Z. This hypothesis appears to be true for the nontransition metals,[1] and for the transition metals it is supported by new experimental results for high-purity single crystals of Mo, Nb, and Ta. These are illustrated in Fig. 1, together with published data for W,[3] Pt,[4,5] and Rh.[5] (See Table I.) The even-Z metals Mo, W, and, for general field and current orientations, Pt exhibit approximately quadratic variation

Table I. Published data for the transition metals.

	Z	Lattice	$\mathfrak{r}$	T (°K)	θ_D(°K)[a]	Sample axis
Mo	42	bcc	1570	2.16	380	4° to [001]
Nb	41	bcc	340	10.6	250	near [110]
Ta	73	bcc	208	2.16	230	random
W[b]	74	bcc	1405	20	315	near [111]
			465	20	315	near [001]
Pt[c]	78	fcc	1400	4.2	225	10° to [001]
Pt[d]			395	4.2	(240)	polycrystal
Rh[d]	45	fcc	500	4.2	(370)	polycrystal

[a] See reference 7.
[b] See reference 3.
[c] See reference 4.
[d] See reference 5.

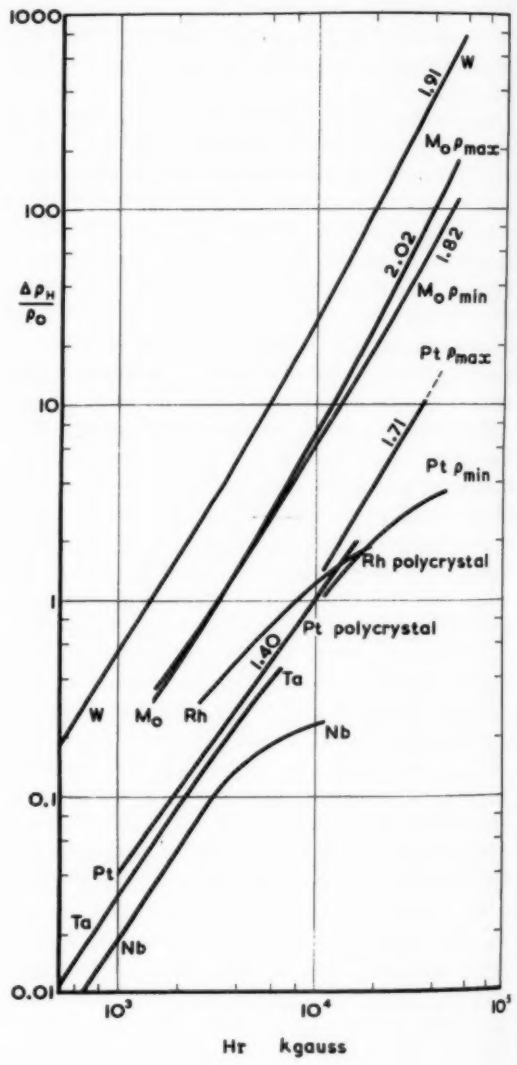

FIG. 1. Magnetoresistance of transition metals. The fractional change in resistivity, $\Delta\rho_H/\rho_0 = (\rho_H - \rho_0)/\rho_0$, is plotted against reduced magnetic field $H\mathfrak{r}$, where $\mathfrak{r} = \rho_0(\theta_D)/\rho_0(T)$ and θ_D is the Debye temperature (Kohler diagram). The exponent m in the expression $\Delta\rho_H/\rho_0 = CH^m$ is shown when the logarithmic plot is linear at the highest fields.

of the resistivity with field which indicates an even number of conduction electrons, while the odd-Z metals Nb and Rh approach saturation at the highest fields. For Ta (odd Z) the highest reduced field[6] $H\tau$ achieved may still be too low to show the onset of saturation.

Single crystals of Mo with current directions near [001], [112], and [110] have been measured in a transverse magnetic field. As the field is rotated about the current direction the resistivity exhibits a marked anisotropy, which is illustrated for a [001] sample in Fig. 2. The field dependence of the resistivity is measured in the direction of minima and maxima, and is always linear on a logarithmic plot at the highest fields (as illustrated for the [001] sample in Fig. 1), the exponent m ranging from 1.75 to 2.04. The absence of cusp-like minima with saturating resistivity shows that open orbits do not occur, which suggests that all sheets of the Fermi surface are simply connected. Further, this behavior being characteristic of even-valent metals for which $\omega_c\bar{\tau} \gg 1$ for all sheets, it is probable that the mobilities of charge carriers in the s and d bands are of the same order of magnitude. The same conclusions are true for W, and the close resemblance of the anisotropy of its magnetoresistance[8] to that of Mo suggests that the shape of the Fermi surface is very similar for the two metals.

The anisotropy of the magnetoresistance for the [001] sample of Pt,[4] shown in Fig. 2, is also superficially similar to that for Mo. But for Pt there is a cusp-like minimum when the field is in the [100] direction, where the resistivity saturates as illustrated in Fig. 1 (curve ρ_{min}). For the other field directions the resistivity rises approximately quadratically at the highest fields (curve ρ_{max}). This behavior indicates an even number of conduction electrons with one (or more) sheets of the Fermi surface multiply connected and giving rise to open orbits for appropriate field directions.

The resistivity for both the Nb and Ta samples in a field $H \sim 30$ kgauss is isotropic to within a few percent, indicating closed Fermi surfaces. The odd-valent behavior of the Nb samples is not conclusive evidence of a noneven number of conduction electrons, since the high electronic specific heat suggests that the effective mass of charge carriers in the d band is high so that perhaps $\omega_c\bar{\tau} < 1$ even at the highest fields. Measurements on purer samples or at higher fields showing continued saturation of the resistivity for Nb and other odd-Z metals would confirm the proposed correlation between Z and the number of conduction electrons.

The author is indebted to Mr. J. A. Belk (Armaments Research and Development Establishment, England) for supplying two Mo samples and to Dr. J. G. C. Milne (University of Bristol, England) for the Ta sample. Other Mo samples and the Nb sample were supplied by Metals Research Ltd., Cambridge, England. Mr. W. H. Mitchell provided helpful technical assistance.

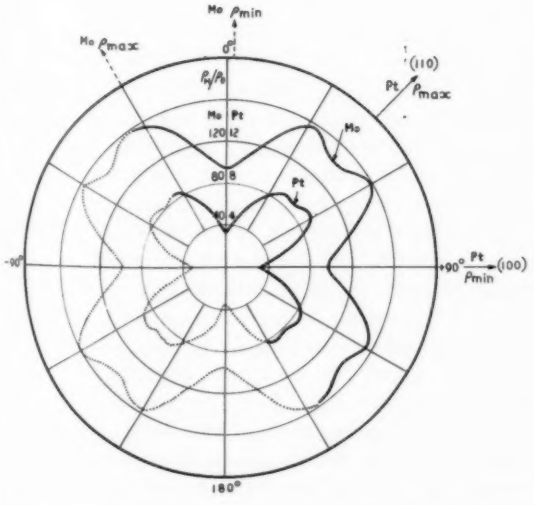

FIG. 2. Anisotropy of the magnetoresistance for Mo and Pt.[4] Mo—outer curve, $H = 31.3$ kgauss, $T = 2.16$°K; Pt (reference 4)—inner curve, $H = 23.5$ kgauss, $T = 4.2$°K. The data for these samples are given in Fig. 1 and Table I, where the field dependence of the resistivity in the directions ρ_{max} and ρ_{min} is illustrated.

---

*Present address: Bell Telephone Laboratories, Murray Hill, New Jersey.

[1]E. Fawcett, Phys. Rev. Letters 6, 534 (1961).

[2]This statement is strictly correct only for metals having simple translation lattices, as have all the metals considered here. For a metal having s atoms in the primitive unit cell sZ determines the even- or odd-valent character of the magnetoresistance. For example, Ga, which is trivalent with $Z = 31$, has an orthorhombic lattice with $s = 8$. Thus sZ is even and the resistivity correspondingly increases quadratically to the highest fields for general field and current orientations [J. Yahia and J. A. Marcus, Phys. Rev. 113, 137 (1959)]; Professor Marcus informs the author that recent measurements by W. A. Reed show a saturating resistivity indicating open orbits for some orientations).

[3]J. De Nobel, Physica 23, 349 (1957).

[4]N. E. Alekseevskii and Yu. P. Gaidukov, J. Exptl. Theoret. Phys. (U.S.S.R.) 38, 1720 (1960) [translation:

Soviet Phys.—JETP 38(11), 1242 (1960)].

[5]R. Schulze, Physik. Z. 42, 297 (1941).

[6]Note that $H\tau=(m_c/e\tau_{\theta_D})\omega_c\bar{\tau}$, m_c being an average cyclotron effective mass and τ_{θ_D} the electron relaxation time at the Debye temperature, which is roughly the same for different metals [but see J. Ziman, Electrons and Phonons (Clarendon Press, Oxford, 1960), p. 492].

[7]G. K. White and S. B. Woods, Phil. Trans. Roy. Soc. (London) A251, 35 (1959).

[8]E. Justi and H. Scheffers, Physik. Z. 37, 700 (1936).

EXPERIMENTAL EVIDENCE OF BIREFRINGENCE BY FREE CARRIERS IN SEMICONDUCTORS

K. J. Schmidt-Tiedemann
Philips Research Laboratory Hamburg, Hamburg, Germany
(Received October 9, 1961)

Recently it has been proposed[1] that the free carriers in a semiconductor should exhibit optical birefringence if their effective mass, averaged over the ensemble of carriers, is anisotropic. It is the purpose of this Letter to present experimental evidence of this effect.

In general, the free carriers in a semiconductor make a contribution, due to their polarizability, to the relative dielectric constant of the crystal which, in the infrared region, is given by

$$\epsilon_F = -(e^2/\epsilon_0\omega^2)n\langle 1/m\rangle. \quad (1)$$

Here e is the electronic charge, ϵ_0 the dielectric constant of free space, ω the angular frequence of the light wave, n the carrier density, and $\langle 1/m\rangle$ the average of the reciprocals of the effective masses of the carriers. Equation (1) is based on several approximations which are discussed by various authors.[2-4]

The average effective mass can be made anisotropic, for example, by disturbing the equipopulation of the sub-bands in a many-valley semiconductor by means of an electric or a strain field.

The present experiments have been carried out with strained n-type germanium. The free-carrier birefringence should reveal itself by a contribution to the stress optical constant Q_{44}, which is given by

$$Q_{44} = \Delta/dX. \quad (2)$$

Here Δ is the relative phase shift of the two light waves in the crystal, d the thickness of the crystal in the direction of the light beam, and X the magnitude of an uniaxial tensile stress in the $\langle 111\rangle$ direction. The wave normal of the radiation must be perpendicular to the stress axis. The other stress optical constant, $Q_{11}-Q_{12}$, should, to a first approximation, remain unaltered by intervalley transitions. The free-carrier effect enters into this quantity only by an isotropic change of the refractive index of the crystal.

In order to obtain an expression for the contribution of the free carriers to the birefringence of the strained crystal, we started with Eq. (1) and evaluated $\langle 1/m\rangle$ by the usual deformation potential formalism. Then we evaluated the stress optical constants from the anisotropic part of the dielectric tensor.[5] It turns out that the stress optical constant Q_{44} is the sum of a contribution due to the lattice, denoted by $Q_{44}{}^L$, and a free-carrier part according to

$$Q_{44} = Q_{44}{}^L - AnT^{-1}F_{1/2}'(\eta_0)/F_{1/2}(\eta_0), \quad (3)$$

where

$$A = e^2[(m_0/m_t)-(m_0/m_l)]\Xi_u S_{44}\lambda/(36\pi\epsilon_0 m_0 c^2 k n_0). \quad (4)$$

Here T is the absolute temperature, m_0 the free-electron mass, m_t and m_l the transverse and longitudinal effective mass, respectively, Ξ_u the deformation potential constant and S_{44} the elastic compliance for uniaxial shear, c the velocity and λ the vacuum wavelength of the light, k the Boltzmann constant, and n_0 the refractive index of the doped crystal. $F_{1/2}(\eta_0)$ is the Fermi integral[6] of order 1/2, and the argument η_0 is the position of the Fermi level with respect to the conduction band minima in the unstrained crystal. $F_{1/2}'$ is the derivative of $F_{1/2}$. In the limiting case of small electron densities or high temperatures Maxwellian statistics applies, and in Eq. (3) the factor $F_{1/2}'/F_{1/2}$ is then replaced by unity. Absorption effects by free carriers have been neglected in the above analysis.

For the numerical calculations, the following values for the parameters involved have been used: 1.435×10^{-6} kg^{-1} cm^2 for the elastic compliance S_{44},[7] and the cyclotron resonance values[8]

for the effective-mass parameters.

The measurements were carried out with infrared radiation of a vacuum wavelength of $2.2 \pm 0.05\ \mu$. The thickness d of the n-type germanium samples in the direction of the light beam was 2 mm. An uniaxial tensile stress up to 300 kg/cm^2 was applied along the $\langle 111 \rangle$ direction. The phase shift was detected by means of a Senarmont-type compensator, and Q_{44} was derived from Eq. (2). Details of the apparatus have been given elsewhere.[9]

Figure 1 shows the experimental results. The uppermost curve (1), taken from an undoped sample, represents the normal photoelasticity of the germanium lattice which is nearly independent of temperature. The following curves are enumerated in the order of increasing doping density.

In order to check the quantitative agreement between theory and experiment, the carrier density n has been determined by Hall measurements.

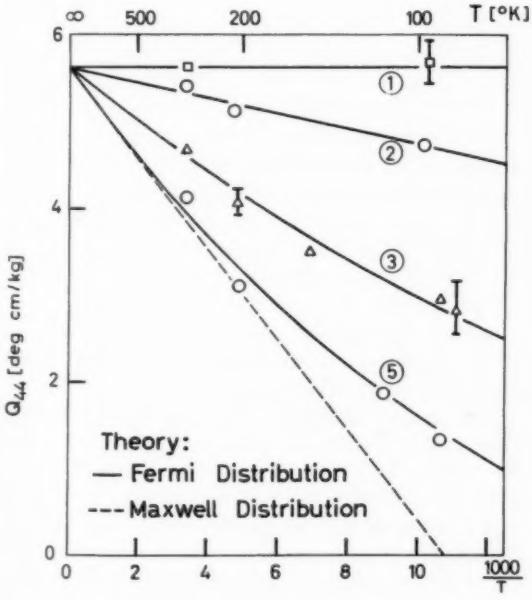

FIG. 1. Temperature dependence of the stress optical constant Q_{44} for n-type germanium samples of different carrier densities. The curves are denoted by the same numbers as their corresponding samples in Table I. The full lines are theoretical curves calculated from the data given in Table I by means of Eqs. (3) and (4). For the sake of clarity, the curve corresponding to sample (4) has been omitted. The broken line represents a calculated relationship corresponding to sample (5) assuming a Maxwellian carrier distribution function.

Additionally, it has been calculated from the resistivity using the resistivity vs carrier density relationship established by Furukawa[10] by means of Hall measurements. The ratio of Hall to drift mobility has been set equal to 0.926 for the samples (2) and (3) corresponding to Maxwellian statistics,[11] and equal to 0.784 for the samples (4) and (5) corresponding to strong degeneracy.[11] The influence of impurity scattering, though presumably not negligible in this range of carrier densities, has not been taken into account.

From these carrier density values and the measured stress optical constants, the deformation potential constant Ξ_u has been calculated by means of Eq. (3) for a lattice temperature of 90°K. The results as given in Table I yield a value of 18.9 $\pm$ 1.7 ev, which is in fair agreement with Fritzsche's value of 18.5 ev determined from piezoresistance measurements.[12] Additionally, the full curves in Fig. 1, which have been calculated from Eq. (3) using corresponding values of n and Ξ_u, give a satisfying representation of the temperature dependence of Q_{44}. We regard this agreement between theory and experiment as a confirmation of the proposed concept of free-carrier birefringence.

If the Maxwellian approximation is introduced for the carrier distribution function, we get a good fit for the sample (2). However, this approximation obviously fails to apply for more strongly doped samples, as can be seen from the broken line in Fig. 1 which corresponds to sam-

Table I. Resistivities ρ in 10^{-3} ohm cm, carrier densities n_H in 10^{18} cm^{-3}, and deformation potential constants Ξ_u in ev as derived from birefringence measurements, for different n-type germanium samples. All data are taken with antimony-doped samples.

Sample	ρ	n_H [a]	n_H [b]	Ξ_u [c]	Ξ_u [d]
(1)	$>10^3$	...	...	...	...
(2)	17.7	0.20	...	20.6	...
(3)	7.3	0.89	0.74	17.8	20.6
(4)	5.1	1.26	1.1	16.4[e]	18.3
(5)	4.6	1.33	1.26	17.2	18.5

[a] Author's Hall measurements.
[b] Furukawa's data (reference 10).
[c] Calculated from values of n_H given in the third column.
[d] Calculated from values of n_H given in the fourth column.
[e] This sample showed strong inhomogeneities of impurity distribution.

ple (5) assuming Maxwellian statistics.

In these considerations, no explicit dependence on temperature of the carrier density has been taken into account. This is, at least for the samples (4) and (5), justified by the fact that the donor ionization energy tends to disappear for donor densities of the order of 10^{18} cm^{-3}.

Extending these measurements to longer wavelengths would increase their sensitivity as well as their accuracy for two reasons: First, the free-carrier effect increases proportionally to λ as long as relaxation effects may be neglected; and second, the lattice birefringence decreases as λ^{-1} in the absence of dispersion. Thus an improvement of the ratio of the electronic to the lattice contribution to birefringence proportional to λ^2 can be obtained. Experiments in this direction are in progress.

The author is indebted to Professor D. Polder, Dr. H. J. G. Meyer, and Dr. N. J. Harrick for stimulating discussions, to Miss I. Ruether and D. Restorff for carrying out the optical and the Hall measurements, and to A. Hauptmann who prepared the crystals.

[1]K. J. Schmidt-Tiedemann, Z. Naturforsch. 16a, 639 (1961).
[2]W. G. Spitzer and H. Y. Fan, Phys. Rev. 106, 882 (1957).
[3]D. Pines, Solid-State Physics, edited by F. Seitz and D. Turnbull (Academic Press, Inc., New York, 1955), Vol. 1, p. 367.
[4]M. Cardona, W. Paul, and H. Brooks, Helv. Phys. Acta 33, 329 (1960).
[5]F. Pockels, Lehrbuch der Kristalloptik (B. G. Teubner, Leipzig and Berlin, Germany, 1906).
[6]J. McDougall and E. C. Stoner, Phil. Trans. Roy. Soc. (London) A237, 67 (1938).
[7]H. J. McSkimin, J. Appl. Phys. 24, 988 (1953).
[8]R. N. Dexter, H. J. Zeiger, and B. Lax, Phys. Rev. 104, 637 (1956).
[9]K. J. Schmidt-Tiedemann, J. Appl. Phys. 32, 2058 (1961).
[10]Y. Furukawa, J. Phys. Soc. Japan 16, 687 (1961).
[11]C. Herring and H. Vogt, Phys. Rev. 101, 944 (1956).
[12]H. Fritzsche, Phys. Rev. 115, 336 (1959).

INTERPRETATION OF THE ELECTROMAGNETIC RADIATION FROM ELECTRON PASSAGE THROUGH METAL FILMS

V. P. Silin and E. P. Fetisov
P. N. Lebedev Physical Institute, Moscow, U.S.S.R.
(Received October 18, 1961)

Recently two interesting experiments[1,2] were published, in which the electromagnetic radiation arising from the passage of fast electrons (25 kev) through thin (450-1500 A) silver films was investigated. At the light wavelength $\lambda = 3300 \pm 100$ A, the spectral distribution of the radiation was found to have a comparatively sharp peak. The strength of the peak proved to be a periodically varying function of the film thickness. Finally, the angular distribution of the radiation was investigated.

Interpreting their experimental results, the authors of those papers[1,2] consider them as corroboration of the theory of plasmons and, in particular, of the theoretical work by Ferrell[3] in 1958. In this communication we try to show that the observed electromagnetic radiation[1,2] is the transition radiation predicted by Ginzburg and Frank[4] as far back as 1946. At the same time, the regularities of the transition radiation detected in the experiments[1,2] are well described by the formula for the spectral and angular distributions of the transition radiation produced by the electrons passing through the film (normally to its surface) which was obtained by Pafomov[5] (see also Garibian and Chalikian[6]). For nonrelativistic particles and not very large values of the dielectric permeability, this formula takes the form

$$dW = (2e^2v^2/\pi c^3)d\omega d\theta \sin^3\theta \cos^2\theta |A(\omega,\theta)|^2, \quad (1)$$

$$A(\omega,\theta) = (\epsilon - 1)[(x+y)e^{-i\omega xd/c} + (x-y)e^{i\omega xd/c} - 2xe^{i\omega d/v}][(x+y)^2 e^{-i\omega xd/c} - (x-y)^2 e^{i\omega xd/c}]^{-1}, \quad (2)$$

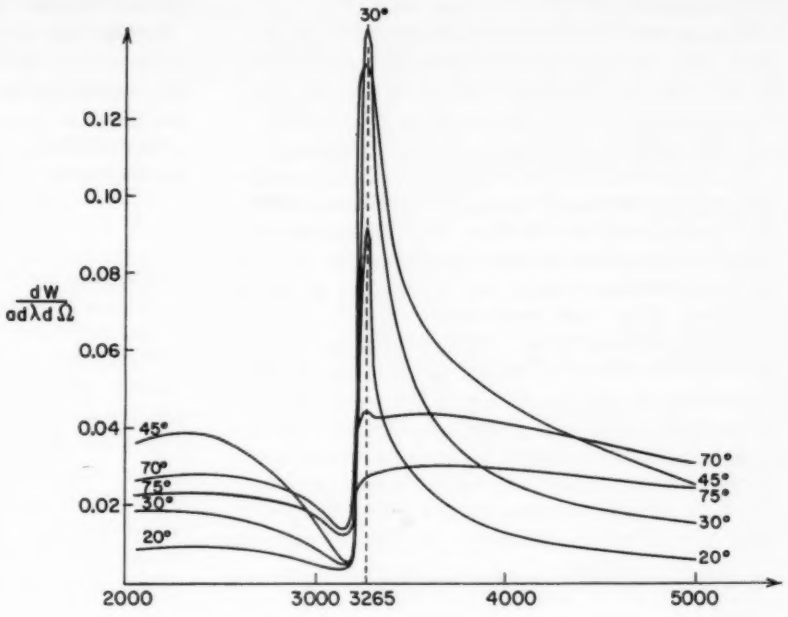

FIG. 1. Dependence of the radiation intensity on the wavelength λ calculated for a series of values of the angle θ at the following parameter values: $d = 500$ A, $v/c = 0.285$. (Coefficient $a = 2e^2v^2/\pi c^3$.)

$$x = (\epsilon - \sin^2\theta)^{1/2}, \quad y = \epsilon \cos\theta. \tag{3}$$

Here $\epsilon(\omega)$ is the complex dielectric permeability, corresponding to a field dependence on the time of $e^{-i\omega t}$. d is the film thickness.

For silver films the Wood transparency arises at the light wavelength of ~3400 A. Near such a wavelength and at not very large angles θ (for example, under conditions of the experiment of reference 2), and when $d = 500$ A, the parameter $(xd\omega/c)$ is small. Then the formula (1) can be written in the following form:

$$dW = (2e^2v^2/\pi c^3)d\omega d\theta \sin^3\theta \cos^2\theta \sin^2(\omega d/2v)$$

$$\times \left| \frac{\epsilon - 1}{\epsilon \cos\theta - i(\omega d/2c)(\epsilon - \sin^2\theta + \epsilon^2 \cos^2\theta)} \right|^2. \tag{4}$$

Now if one takes into account the fact[7] that the imaginary part of the dielectric permeability of silver near $\lambda = 3400$ A is approximately equal to 0.2-0.3, then one finds that Eq. (4) gives an angular distribution of the experimentally detected radiation (Fig. 2 of reference 2), an oscillatory dependence of the radiation intensity on film thickness with the period $(\omega d/v)$ (reference 1), and also a spectral distribution of the radiation which all have the right behavior to agree with experiment.

Since $(\omega x d/c)$ is not a small value in the whole region of frequencies and film thicknesses studied experimentally, we have in fact used Eqs. (1) and (2) for computing the yields shown in Figs. 1 and 2. It will be seen that these are in good agreement with the experiments. The values of the optical constants used in obtaining the graphs were taken

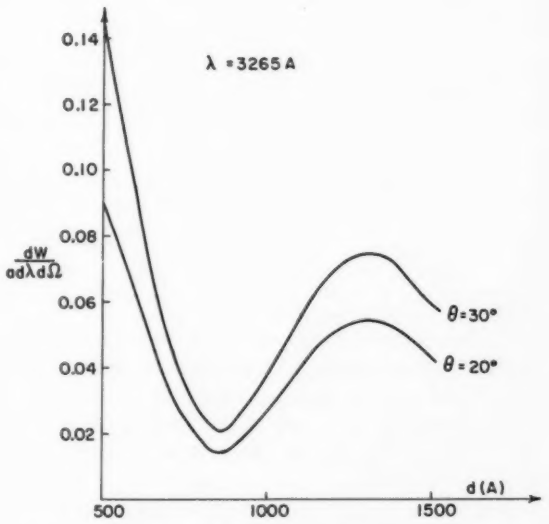

FIG. 2. Dependence of the radiation intensity on the film thickness calculated for the angles $\theta = 30°$ and $\theta = 20°$. (v/c and a are the same as in Fig. 1.)

from reference 7.

In the theory of transition radiation[4-6] it is assumed that only transverse waves can propagate in the medium. For investigation of propagation of longitudinal waves (plasmons) in the medium one must take into account a spatial dispersion of the dielectric permeability.[8] Since in this case existence of waves of three polarizations proves to be possible in the medium, it is necessary to make certain physical statements equivalent to additional boundary conditions,[9-11] in order to obtain solutions of the field equations.

In this communication, the following model was used for revealing the role of longitudinal waves (plasmons) for the conditions of the experiments.[1,2] Since in the conditions under consideration the product of the wavelength vector k of a light wave by the characteristic velocity of the electron is small in comparison with the frequency and we deal with the region around the Wood transparency, one can consider a weak spatial dispersion.[8,9]

In this case a spatial dispersion of the transverse dielectric permeability, owing to its small value, was neglected, and the longitudinal permeability was taken in the form: $\epsilon^{l}=\epsilon-\alpha(k/\omega)^2$. The value α, for example, in the model of free electrons, has the form

$$\alpha=\tfrac{3}{5}v_0^{\,2}\omega_L^{\,2}/\omega^2,$$

where v_0 is the velocity of electrons on the Fermi surface and ω_L is the Langmuir frequency of electrons.

The following boundary condition was used: The normal component of the field of the radiation going inside the metal is equal to zero on the surface. Such a boundary condition was obtained by a microscopic consideration of the problem of oblique incidence of the electromagnetic wave on a semi-infinite medium where the electrons of the medium suffer a mirror reflection at the surface.[10]

Then, instead of the formula (2), we obtain

$$\frac{\epsilon}{\epsilon-\alpha/v^2}(\epsilon-1-\alpha/v^2)\Big\{(x+y)e^{-i\omega xd/c}+(x-y)e^{i\omega xd/c}-2xe^{i\omega d/v}+\frac{\sin^2\theta}{z}\Big[e^{-i\omega xd/c}-e^{i\omega d/v}+e^{i\omega zd/c}$$

$$-e^{i\omega d/v+i\omega zd/c-i\omega xd/c}\Big]\Big\}\Big\{(x+y)^2e^{-i\omega xd/c}-(x-y)^2e^{i\omega xd/c}+2\frac{\sin^2\theta}{z}\Big[(y-x)e^{i\omega zd/c}+(x+y)e^{-i\omega xd/c}\Big]$$

$$-\frac{\sin^4\theta}{z^2}\Big[e^{2i\omega zd/c-i\omega xd/c}-e^{-i\omega xd/c}\Big]\Big\}^{-1}, \tag{5}$$

where $z=[\epsilon(c^2/\alpha)-\sin^2\theta]^{1/2}$.

The origin of the expression $\epsilon-\alpha/v^2$ in the formula (5) which makes, in particular, this formula different from formula (2), depends on the fact that, in taking into account the spatial Fourier expansion of the charge field, it is proportional to $1/[\epsilon-\alpha(k/\omega)^2]$.

Since α is roughly equal to the square of the Fermi electron velocity ($v_0\sim10^8$ cm/sec), it is obvious that at the incident electron energy of ~25 kev the value (α/v^2) is equal to the order of 10^{-4} and cannot be discerned in the experiments.[1,2] That is why it is impossible to see the change of form caused by the Coulomb field. It is clear that for revealing such an effect, it is necessary to make the energy of the incident electrons considerably less, and, also, to use targets with a smaller imaginary part of the dielectric permeability; for example, the alkali metals. Another distinction of formula (5) from formula (2) involves the terms proportional to $1/z$ and $1/z^2$. Note here that any changes in the boundary conditions lead to modifications in the coefficients in front of such terms. Nevertheless, the order of magnitude does not change.[12] On the other hand, since in our conditions z is rather large (namely, $z\sim100$), for revealing the role of terms $1/z$ in the formula (5), measurements with an accuracy of about a percent are necessary. The main dependence of the radiation arising from electrons passing through the metal film on frequency, angle, and film thickness is determined, in the conditions of the experiments,[1,2] by the formulas (1) and (2).[13]

Thus, consideration of the possibility of propagation of longitudinal waves (plasmons) in the matter and also the possibility of their transformation into transverse electromagnetic waves radiating

into vacuum does not lead, in the conditions of the experiments,[1,2] to effects which are appreciable compared to the transition radiation, the theory of which agrees with the experimental results.[1,2]

The authors wish to thank V. L. Ginzburg and I. M. Frank for interest in the work and also L. V. Parijskaya for preparing the graphs.

[1]W. Steinmann, Phys. Rev. Letters 5, 470 (1960).
[2]R. W. Brown, P. Wessel, and E. P. Trounson, Phys. Rev. Letters 5, 472 (1960).
[3]R. A. Ferrell, Phys. Rev. 111, 1214 (1958).
[4]V. L. Ginzburg and I. M. Frank, J. Exptl. Theoret. Phys. (U.S.S.R.) 16, 15 (1946).
[5]V. E. Pafomov, J. Exptl. Theoret. Phys. (U.S.S.R.) 33, 1074 (1957) [translation: Soviet Phys. - JETP 6(33), 829 (1958)].
[6]G. M. Garibian and G. A. Chalikian, J. Exptl. Theoret. Phys. (U.S.S.R.) 35, 1282 (1958) [translation: Soviet Phys. - JETP 35(8), 894 (1959)].
[7]E. A. Taft and H. R. Philipp, Phys. Rev. 121, 1100 (1961).
[8]A. A. Rukhadze and V. P. Silin, Electromagnetic Properties of Plasma and Plasma-Like Media (Atomizdat, U.S.S.R., 1961).
[9]V. L. Ginzburg, J. Exptl. Theoret. Phys. (U.S.S.R.) 34, 1954 (1958).
[10]V. P. Silin and E. P. Fetisov, J. Exptl. Theoret. Phys. (U.S.S.R.) 41, 159 (1961) [translation: Soviet Phys. - JETP (to be published)].
[11]V. L. Zhelnov, J. Exptl. Theoret. Phys. (U.S.S.R.) 40, 170 (1961) [translation: Soviet Phys. - JETP 13, 117 (1961)].
[12]Compare, for example, with reference 11.
[13]This result agrees with the conclusion obtained in reference 11 for transition radiation from one boundary.

$K^+ + d$ CHARGE-EXCHANGE REACTION FROM 52 TO 456 Mev*†

William Slater, Donald H. Stork, and Harold K. Ticho
Physics Department, University of California, Los Angeles, California
and
Wonyong Lee, William Chinowsky, Gerson Goldhaber, Sulamith Goldhaber, and Thomas O'Halloran
Physics Department and Lawrence Radiation Laboratory, University of California, Berkeley, California
(Received October 23, 1961)

Below the threshold for π-meson production the K^+ meson interacts strongly with nucleons by the following three processes:

Reaction	Scattering amplitude	
$K^+ + p \to K^+ + p$,	$f_1 + f_C$;	(1a)
$K^+ + n \to K^+ + n$,	$\frac{1}{2}(f_1 + f_0)$;	(1b)
$K^+ + n \to K^0 + p$,	$\frac{1}{2}(f_1 - f_0)$.	(1c)

These processes can be described by the Coulomb scattering amplitude f_C and the two charge-independent scattering amplitudes f_0 and f_1, corresponding to the total isotopic spin 0 and 1, respectively.[1]

Elastic $K^+ + p$ scattering experiments give information on the f_1 amplitude. Information on the f_0 amplitude has in the past been obtained from the charge-exchange (CE) scattering of K^+ mesons in complex nuclei.[2,3] These measurements led to determination of total charge-exchange cross sections per neutron, to evidence for p-wave scattering in the $T=0$ state, and to crude angular distributions of the K^0 mesons.[4] In this work we study the charge-exchange scattering of K^+ mesons on deuterons, in the Lawrence Radiation Laboratory 15-inch bubble chamber filled with deuterium. The chamber was exposed to a highly separated K^+-meson beam,[5] at six different energies: 52, 100, 127, 230, 315, and 456 Mev. For the determination of the charge-exchange cross section we have selected those events giving a subsequent charged decay mode for the K_1^0 meson. This sample corresponds to $\frac{2}{3}$ of all K_1^0 decays and thus to $\frac{1}{3}$ of all charge-exchange events (both K_1^0 and K_2^0 production).[6]

The K^+-meson path length was obtained by two independent methods[7]: (a) by direct measurements of the K^+ tracks in every tenth picture; and (b) by inferring the total path length from the number of "τ-like" decays.[8]

In Table I we list the charge-exchange cross section on deuterium at the six different energies along with the number of events we observed at each energy. In Fig. 1 we show the same cross sections as a function of K^+ kinetic energy in the laboratory system. The scattering angle in the K^+n c.m. system was calculated by assuming (a) an initially stationary neutron, and (b) a neutron initially moving with a momentum equal and opposite to that of the observed or inferred spectator proton. The momentum of the spectator proton was obtained for each event either by direct observation or by kinematical fitting[9] to the reaction

$$K^+ + d \to K^0 + p + p_{\text{spect}}. \quad (2)$$

These two different methods gave essentially identical angular distributions. In Figs. 2(a), (b), (c), and (d) we show the observed differential CE cross sections in the laboratory system. In Figs. 2(a′), (b′), (c′), and (d′) we show the same data transformed to the K^+n c.m. system. The curves shown are calculated fits from a phase-shift analysis discussed below in detail.

Table I. The total $K^+ + d$ charge-exchange (CE) cross sections at various energies and the number of charge-exchange events with subsequent charged K_1^0 decay at each energy.

T (Mev)	Number of CE events	σ_{Kd} for CE (mb)
52 ±17	13	$1.0^{+0.4}_{-0.3}$
100 ±13	46	2.7 ±0.4
127 ±11	65	3.1 ±0.4
230 ±11	161	6.5 ±0.6
315 ± 6	216	6.7 ±0.6
456 ± 5	196	6.6 ±0.7

In order to extract the information on the $K^+ + n$ charge-exchange reaction (1c) from the $K^+ + d$ charge-exchange reaction (2), we use the impulse and closure approximations. The validity of the impulse approximation in this work is examined in two ways[10]: (a) We compare the momentum distribution of the spectator protons with the nucleon momentum distribution in the deuterons as given by the Hulthén wave function. The two are in excellent agreement with each other. (b) We compare the K^0 angle and momentum for each individ-

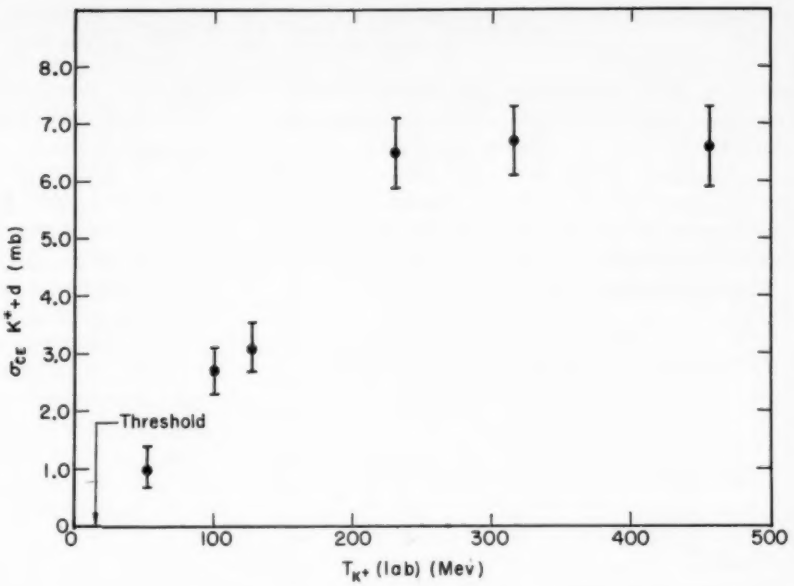

FIG. 1. The $K^+ + d$ charge-exchange cross section as a function of the K^+ energy.

ual event with the two-body kinematics corresponding to Reaction (1c). With few exceptions, the individual points form a band ± 50 Mev/c around the curve given by the two-body kinematics.

For Reactions (2), the impulse and closure approximations give[11]

$$d\sigma/d\Omega = (1/4k^2)\{[\,|a_1 - a_0|^2 + \tfrac{2}{3}|b_1 - b_0|^2][1 - H_2(\theta)] + \tfrac{1}{3}|b_1 - b_0|^2[1 + H_2(\theta)]\}. \quad (3)$$

Here all quantities are computed in the c.m. system of a K meson and a stationary neutron,

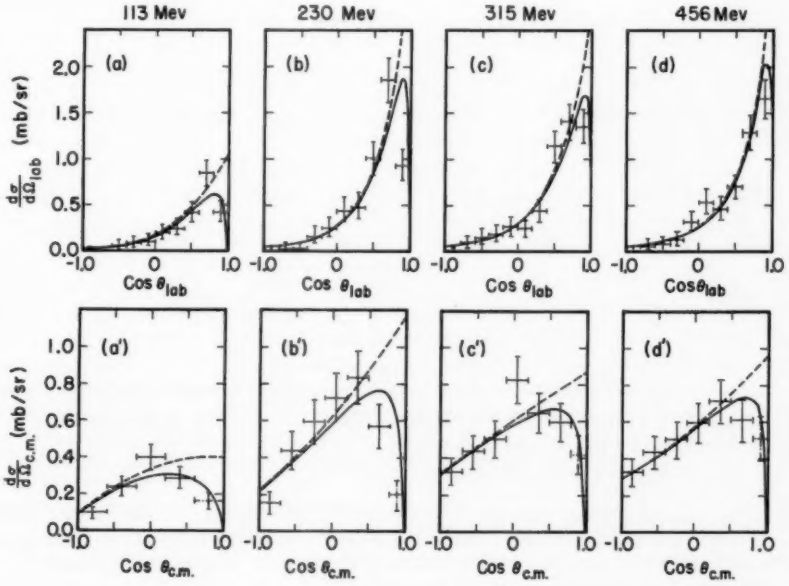

FIG. 2. The differential $K^+ + d$ charge-exchange cross sections at a series of K^+ energies. Figures 2(a), (b), (c), and (d) show the differential cross sections in the laboratory system. Figures 2(a'), (b'), (c'), and (d') show the same cross sections in the c.m. system of K^+ and an initially moving neutron with momentum equal and opposite to the "spectator" proton. The solid curves were computed from the phase-shift solutions with $T=1$ s wave and $T=0$ s and p waves (Solution A, Table II). The dashed curves come from the same solutions, setting $H_2(\theta) \equiv 0$, and thus correspond to the scattering from free neutrons.

$$H_2(\theta)=\frac{2(\alpha+\beta)\alpha\beta}{(\alpha-\beta)^2}\frac{1}{K}\left[\tan^{-1}\left(\frac{K}{2\alpha}\right)-2\tan^{-1}\left(\frac{K}{\alpha+\beta}\right)+\tan^{-1}\left(\frac{K}{2\beta}\right)\right], \quad (4)$$

where in (4) we approximate K, the momentum transfer in the lab system, by the nonrelativistic value $K\approx 2k\sin(\theta/2)$. This approximation is very good for small values of θ. For large values of θ the function $H_2(\theta)$ is small and insensitive to K. The quantities $\alpha=45.5$ Mev and $\beta=7\alpha$ come from use of the Hulthén wave function for the deuteron.

For each isotopic spin we have

$$a_T(\theta)=\sum_{l=0}^{l_{\max}}\{(l+1)\eta_{Tl}^{+}+l\eta_{Tl}^{-}\}P_l^0(\theta),$$

$$b_T(\theta)=i\sum_{l=1}^{l_{\max}}\{\eta_{Tl}^{+}-\eta_{Tl}^{-}\}P_l^1(\theta).$$

Here $\eta_{Tl}^{\pm}$ refers to $j=l\pm\frac{1}{2}$, and $\hbar k$ is the momentum in the K^+n c.m. system.

In the derivation of Eq. (3) the Pauli principle for the two outgoing protons is taken into account. Correction terms due to the final proton-proton interactions, multiple scattering, and the K^+-K^0 mass difference have not been included. These correction terms are likely to contribute most to small scattering angles. In order to test the importance of these neglected terms we have carried out the phase-shift analysis once for the entire angular interval and once for the angular interval $\cos\theta_{\text{c.m.}}<0.6$. Within the errors, the solutions common to the two cases were the same.

We have carried out a phase-shift analysis[12] for

Table II. Phase-shift solutions with errors. Sets A and B are the small and large s-wave solutions in the sp fit. These phase shifts were computed on the assumptions that (a) the $T=1$ state can be expressed as a pure repulsive s wave, and (b) $T=0$ d- and higher angular-momentum waves can be neglected.

T_k (Mev)	Solutions	$T=1$ $S_{1/2}(\delta_1)$ (deg)	$T=0$ $S_{1/2}(\delta_0)$ (deg)	$T=0$ $P_{1/2}(\delta_{01})$ (deg)	$T=0$ $P_{3/2}(\delta_{03})$ (deg)	Probability from χ^2 fit (%)	Cross sections computed from phase shifts: σ_{Kn}, CE (mb)	σ_{Kn}, elastic (mb)	σ_{Kd}, NCE[a] (mb)	Experimental σ_{Kd}, NCE[b] (mb)
				Set A						
113	1	-23	- 6 ± 6	- 7 ± 4	10 ±2	4	4.0 ±0.7	7.9 ±3.1	27	21 ±5
	2			15 ± 4	- 1 ±2					
230	1	-34	13 ± 5	- 4 ± 5	14 ±4	2	8.1 ±0.7	3.8 ±1.0	21	
	2			20 ± 7	2 ±2					
313	1	-41	15 ±10	- 9 ± 7	15 ±7	16	7.5 ±0.5	4.2 ±1.2	20	
	2			23 ±12	- 1 ±2					
456[c]	1	-50	24 ± 4	- 8 ± 3	21 ±3	70	7.5 ±0.4	5.3 ±0.5	19	20 ±2
	2			31 ± 6	2 ±2					
				Set B						
113	1	-23	-33 ± 6	-18 ± 6	4 ±4	20	3.4 ±2.0	24 ±5	47	21 ±5
	2		13 ± 3	-10 ± 4						
230	1	-34	-68 ±12	-26 ±13	15 ±10	50	7.8 ±3.9	29 ±3	45	
	2			29 ±11	-12 ±9					
313	1	-41	-54 ±20	-57 ±15	10 ±8	20	7.3 ±2.7	26 ±5	40	
	2			48 ±15	-19 ±8					
456	1	-50	-76 ±12	-75 ±30	2 ±10	70	6.9 ±1.9	23 ±2	35	20 ±2
	2			59 ±30	-20 ±10					

[a] σ_{Kd}, NCE, the $K+d$ non-charge-exchange cross section, is calculated with a cutoff angle of $\cos\theta_{\text{lab}}=0.94$. Errors in the calculated σ_{Kd}, NCE reflected from errors in phase shifts are ≤3 mb and are not quoted.

[b] The value at $T_K=456$ Mev comes from reference 16. The value quoted at 113 Mev was obtained from our own data[12] at 100 Mev.

[c] An additional large positive $T=0$ s-wave solution exists for this energy with σ_{Kn}, elastic ≈ 12 mb, namely: $\delta_0'=55°$, and $(\delta_{01}',\delta_{03}')=(-9°,+20°)$ or $(+25°,-3.5°)$. Here δ_{01}' and δ_{03}' have the same values (within the errors) as in solutions A_1 and A_2 for 456 Mev above, while δ_0' is related to δ_0 through $|\delta_1-\delta_0'|\approx\pi-|\delta_1-\delta_0|$. The ambiguity observed here always occurs for $|\delta_1-\delta_0|\approx\pi/2$.

the differential cross sections at kinetic energies 113, 230, 315, and 456 Mev. Each energy was treated independently. In our analysis the $T=1$ phase shifts were assumed to be pure s-wave phase shifts[13] and were taken from the $K^+ + p$ data.[14,15] We solved for the $T=0$ phase shifts assuming the scattering process in the $T=0$ state to be (a) s- and p-wave, and (b) s-, p-, and d-wave.

(a) Permitting the scattering to occur in the $T=0$ s and p states leads to two sets of solutions, A and B, each with its Fermi-Yang ambiguity (see Table II). The two solutions A and B differ principally in the sign and magnitude of the $T=0$ s wave. Solutions A and B lead to $K^+ + n$ cross sections which differ from each other by a factor of about four, and $K^+ + d$ non-charge-exchange (NCE) cross sections which differ by a factor of about two. Experimentally we know the total $K^+ + d$ cross sections at two of the energies,[16] and from these obtain values for the $K^+ + d$ NCE cross sections. The values obtained from solution A are in good agreement with those obtained from experiment. Solution B, which gives a better χ^2 fit to the differential CE cross section, can be definitely ruled out because it leads to too large a $K^+ + d$ NCE cross section. We are thus left at each energy with the two Fermi-Yang solution sets A_1 and A_2. The solid curves in Fig. 2 present the differential CE cross section computed from solutions A both in the laboratory and in the center-of-mass systems. The dashed curves were computed from the same phase shifts by setting $H_2(\theta) \equiv 0$ in Eq. (3). The difference between the dashed and solid curves thus illustrates the suppression of the forward scattering due to the Pauli exclusion principle. In Fig. 3 we show the energy dependence of the phase shifts obtained in solutions A_1 and A_2. It is interesting to note that in contrast to the $T=1$ s-wave phase shifts, which are negative (repulsive potential), the $T=0$ s-wave phase shifts are positive (attractive) over the energy interval from about 150 to 456 Mev. From the present data we cannot conclude, however, whether at lower energies δ_0 would remain attractive or turn weakly repulsive.

(b) In an attempt to improve the goodness of fit to our data, we have introduced two more parameters in our phase-shift analysis corresponding to $d_{3/2}$ and $d_{5/2}$ waves.[12] The introduction of these two additional parameters improves the fit somewhat but, as expected from our limited statistics, increases the uncertainty on all values of the phase shifts. The solutions obtained can be divided into three sets, of which two are similar to sets A and B with small d-wave phase shifts added. Here again we can rule out the solution similar to B on comparison with the experimental NCE σ_{Kd}. The third set of solutions tries to fit the data with small negative δ_0 phases, from -5 deg to -15 deg, small p-wave phases, and d-wave phase shifts of which one ranges from -15 deg to -30 deg and the other is small and positive. We must stress, however, that the statistics of our data permit us only to make a first exploration into the domain of higher partial waves which may contribute to the scattering process.

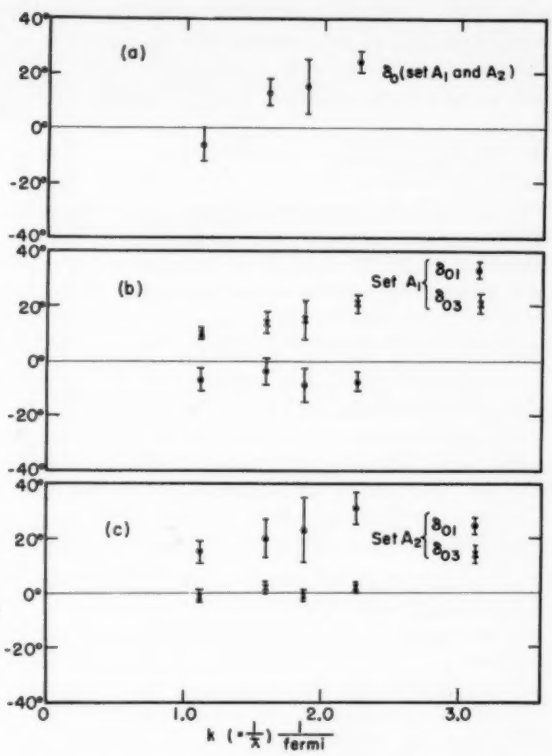

FIG. 3. The phase-shift solution sets A_1 and A_2 (see Table II) as a function of k, the momentum in the $K^+ n$ c.m. system, expressed in inverse fermis (10^{13} cm^{-1}). Not shown in the figure is one further ambiguity in δ_0 at 456 Mev, giving $\delta_0 = 55$ deg. (See Table II, footnote c.)

We wish to thank Professor Luis W. Alvarez and many members of his group for making the 15-inch bubble chamber and analyzing facilities available to us. We are very grateful for the tireless efforts of the bubble chamber crew and the Bevatron crew as well as of our own scanning and measuring group, without whose assistance this

experiment would not have been possible. We would also like to acknowledge the important contributions of Theodore Stubbs and Jean Fisk, as well as helpful discussions with Professor K. M. Watson.

---

*Work submitted in part to the University of California by Wonyong Lee in partial fulfillment of the requirements for the Ph.D. degree.

†This work was done under the auspices of the U. S. Atomic Energy Commission.

[1]In this analysis we consider the K^+ and K^0 mesons to form an isotopic-spin doublet. In this connection, see A. Pais [Phys. Rev. 112, 624 (1958)], who discusses the consequences of K-meson singlets with opposite parity.

[2]M. A. Melkanoff, O. R. Price, D. H. Stork, and H. K. Ticho, Phys. Rev. 113, 1303 (1959); B. Secchi-Zorn and G. T. Zorn, Phys. Rev. 130, 1898 (1960); D. Keefe, A. Kernan, A. Montwill, M. Grilli, L. Guerriero, and G. A. Salandin, Nuovo cimento 12, 241 (1959).

[3]M. N. Whitehead, R. E. Lanou, V. Cook, Jr., and R. W. Birge, Phys. Rev. 118, 300 (1960).

[4]E. Helmy, D. J. Prowse, and D. H. Stork, Nuovo cimento 19, 179 (1961).

[5]G. Goldhaber, S. Goldhaber, T. Kadyk, T. Stubbs, D. H. Stork, and H. K. Ticho, Lawrence Radiation Laboratory Internal Report Bev-483, 1960 (unpublished).

[6]See, for example, F. Crawford, Jr., M. Cresti, R. Douglass, M. Good, G. Kalbfleisch, M. Stevenson, and H. Ticho, Phys. Rev. Letters 2, 266 (1959).

[7]At 52 Mev, Method (a) only was used. At 456 Mev, Method (b) only was used.

[8]By "τ-like" decays we mean K^+ decays into three charged secondaries; these correspond to a fraction $f_1 = 0.061 \pm 0.002$ of all K^+ decays. This number is a weighted average of results quoted by L. B. Okun, Ann. Rev. Nuclear Sci. 9, 61 (1959), and our own measurements on stopping K^+ mesons. In both cases the branching ratio obtained for these decay modes was $f_1 = 0.061 \pm 0.003$.

[9]The spectator proton was identified by comparing the fitted quantities of both protons with a track computed on the assumption of K^+ scattering off a neutron. We found the lower momentum proton to fulfill the properties of the spectator in nearly all of the events, and utilized this method for the selection of the spectator (reference 10). In this work we utilized the geometrical reconstruction (PANG) and kinematical fitting (KICK) programs of the Alvarez Group. J. P. Berge, F. T. Solmitz, and H. D. Taft, Rev. Sci. Instr. (to be published), and A. H. Rosenfeld and J. M. Snyder, Rev. Sci. Instr. (to be published).

[10]The graphs showing these distributions were presented at the 1960 Rochester Conference [W. Chinowsky, G. Goldhaber, S. Goldhaber, W. Lee, T. O'Halloran, T. Stubbs, W. Slater, D. H. Stork, and H. K. Ticho, in Proceedings of the 1960 Annual International Conference on High-Energy Physics at Rochester (Interscience Publishers, Inc., New York, 1960), p. 451.

[11]S. Fernbach, T. Green, and K. Watson, Phys. Rev. 84, 1084 (1951); R. Rockmore, Phys. Rev. 105, 256 (1957); K. Rogers and L. Lederman, Phys. Rev. 105, 247 (1957); E. Ferreira, Phys. Rev. 115, 1727 (1959); and M. Gourdin and A. Martin, Nuovo cimento 11, 670 (1959); 14, 722 (1959).

[12]For details see Wonyong Lee, thesis, Lawrence Radiation Laboratory Report UCRL-9691, 1961 (unpublished).

[13]We have also explored the behavior of the $T = 0$ phase shifts for the case of p waves in the $T = 1$ state. For dominant $T = 1$ $p_{1/2}$ solutions (reference 14) we obtain $T = 0$ solutions which can be identified with the Minami transformations of solutions A and B quoted in Table II. For the $T = 1$ $p_{1/2}$ and $p_{3/2}$ dominant solutions (reference 14) we obtain several solutions by fitting the differential charge-exchange cross section, most of which can be ruled out on comparison with the experimental σ_{Kd}, NCE. At present the evidence for dominant p-wave scattering in the $T = 1$ state is not strong enough to warrant a thorough study of solutions other than those containing pure s wave in the $T = 1$ state.

[14]T. Stubbs, H. Bradner, W. Chinowsky, G. Goldhaber, S. Goldhaber, W. Slater, D. H. Stork, and H. K. Ticho, Phys. Rev. Letters 7, 188 (1961).

[15]T. F. Kycia, L. T. Kerth, and R. G. Baender, Phys. Rev. 118, 553 (1960).

[16]V. Cook, D. Keefe, L. T. Kerth, P. G. Murphy, W. A. Wenzel, and T. F. Zipf, Phys. Rev. Letters 7, 182 (1961). See also footnote in Table II.

EVIDENCE FOR A PION-PION RESONANCE FROM PHOTOPRODUCTION OF PION PAIRS*

D. McLeod, S. Richert, and A. Silverman
Laboratory of Nuclear Studies, Cornell University, Ithaca, New York
(Received October 17, 1961)

In the reaction $\gamma + p \rightarrow \pi^+ + \pi^- + p$, we may expect that the behavior of the cross section will be influenced by interactions between the particles in the final state. We have made measurements of this cross section particularly designed to give evidence concerning the pion-pion interaction.

A difficulty in such an attempt is that the strong pion-proton interaction might obscure any pion-pion effect. Our approach has been that suggested by Drell and Zachariasen.[1] Let $E_{p\pi^+}$, $E_{p\pi^-}$, and $E_{\pi\pi}$ be the total energies of the indicated pairs of particles in the center-of-mass system of each pair. It is possible to vary the parameters of the reaction so that $E_{p\pi^+}$ and $E_{p\pi^-}$ are held constant, while $E_{\pi\pi}$ is varied.[2] Choosing constant values of $E_{p\pi^+}$ and $E_{p\pi^-}$ well away from any pion-proton resonance, it is hoped that the final-state nucleon-pion interaction will be kept small and substantially constant, so that a pion-pion resonance will reveal itself in a "bump" as $E_{\pi\pi}$ is varied.

The reaction is observed by detecting the proton and one of the pions in coincidence, measuring the direction and momentum of each. These parameters completely determine the kinematics, so that k, the incident γ-ray energy, and the momentum of the undetected pion are known. The experimental setup is shown in Fig. 1. The bremsstrahlung beam of the Cornell synchrotron passes through a 3-in. liquid hydrogen target and is monitored by a quantameter.[3] Particles of given direction and momentum are focussed by one of the two magnetic spectrometers, $M1$ and $M2$, into scintillation counter telescopes. Protons are unambiguously identified in $M1$ by pulse-height analysis in three scintillation counters. Pions are detected in $M2$, where protons are eliminated by requiring a Lucite Čerenkov counter in coincidence. A resolving time of 5 nanoseconds is achieved in the coincidence between proton and pion by photographing an oscilloscope trace displaying one signal from each telescope. Background from random coincidences averages about 5%. A given setting of the magnet angles and momenta determines the incident γ-ray energy at which the specified 2-pion reaction will occur; the peak bremsstrahlung energy is then set at a value well above this, but low enough so that no 3-pion process can contribute. For each point measurements are also made with the peak energy somewhat below the 2-pion energy, and this yield (typically 10%) is subtracted as background. Two measurements are made for each condition; one with the $M2$ polarity set to

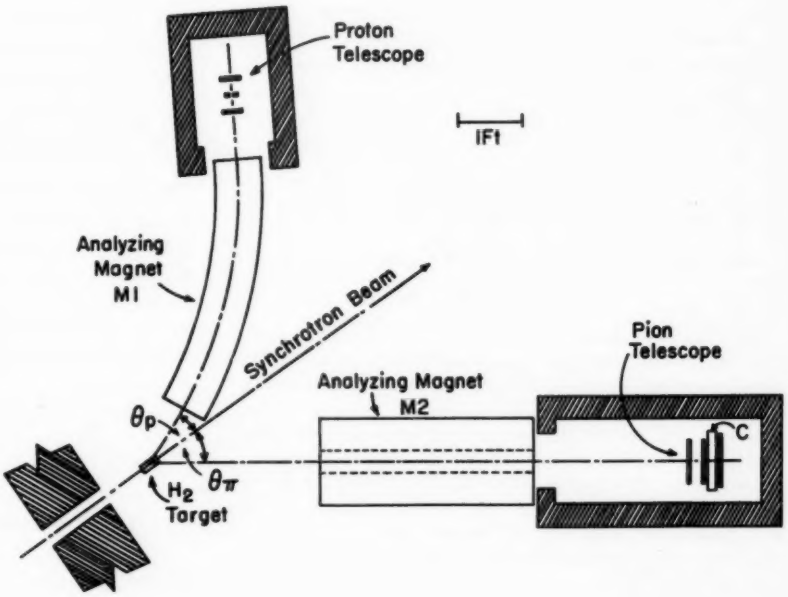

FIG. 1. Experimental setup. $M1$ is a two-lens, strong-focussing, 35° bending magnet, with parameters: $\Delta p/p = 12\%$; $\Delta\Omega = 4 \times 10^{-3}$ sr; $\Delta\theta = 5°$. $M2$ is a Panofsky-Hand type quadrupole magnet [L. N. Hand and W. K. H. Panofsky, Rev. Sci. Instr. 30, 927 (1959)] with a lead barrier in the center, as a momentum spectrometer with a line focus. Its parameters are: $\Delta p/p = 7.5\%$; $\Delta\Omega = 9 \times 10^{-3}$ sr; $\Delta\theta = 2°$. The counter marked C is a Lucite Čerenkov counter; all others are scintillation counters.

accept π^+, and the other for π^-.

Results are expressed in terms of M^2, the square of the invariant matrix element, which is related to the cross section and laboratory phase space, D, as follows. ($\hbar = c = 1$.)

$$d\sigma/(d\Omega_p d\Omega_{\pi 1} dp_p) = 2\pi M^2 D/(32\, k m_p E_p E_{\pi 1} E_{\pi 2}),$$

where

$$D = \frac{E_{\pi 1} E_{\pi 2}}{(2\pi)^6} \frac{p_{\pi 1}{}^3 p_p{}^2}{[p_{\pi 1}{}^2 (k + m_p - E_p) - E_{\pi 1} \vec{p}_{\pi 1} \cdot (\vec{k} - \vec{p}_p)]}.$$

Here k is the incident photon momentum; $\vec{p}$ and E are the laboratory momentum and energy of a final-state particle; the subscript p refers to the proton, π_1 to the detected pion, and π_2 to the other pion. In this form, M^2 has the dimensions of area.

Two series of measurements were made: one with $E_{p\pi 1} = 1.414$ Bev, $E_{p\pi 2} = 1.140$ Bev; a second with $E_{p\pi 1} = 1.414$ Bev, $E_{p\pi 2} = 1.161$ Bev. ($\pi 1$ is the pion detected in $M2$, $\pi 2$ is the other pion.) Figure 2 shows the results of the second series;

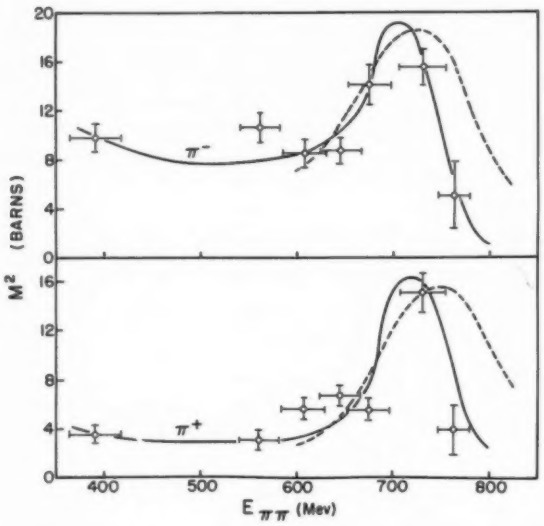

FIG. 2. M^2 vs $E_{\pi\pi}$ for $E_{p\pi^+} = 1.161$ Bev, $E_{p\pi^-} = 1.414$ Bev (upper half); and for $E_{p\pi^+} = 1.414$ Bev, $E_{p\pi^-} = 1.161$ Bev (lower half). In Figs. 2 and 3, errors indicated on M^2 are statistical, except for the special case noted in the text. Horizontal limits show the experimental resolution. The labels π^+, π^- indicate the sign of the detected pion. The curves shown are the results of the model described in the text, with the variation of the π-π phase shift determined to fit our data (solid lines), and determined from reference 4 (dashed lines). (See Fig. 4.)

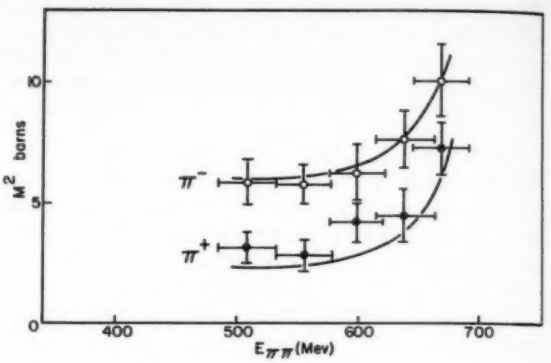

FIG. 3. M^2 vs $E_{\pi\pi}$ for $E_{p\pi^+} = 1.140$ Bev, $E_{p\pi^-} = 1.414$ Bev (open points); and for $E_{p\pi^+} = 1.414$ Bev, $E_{p\pi^-} = 1.140$ Bev (solid points).

Fig. 3, the first series. The labels π^+, π^- indicate the sign of the detected pion. Errors indicated on M^2 are counting statistics, except for the points at $E_{\pi\pi} = 760$ Mev. For these points the γ-ray energy determined by the magnet settings was very close to the peak beam energy. This led to a substantial correction factor critically dependent on the value taken for the beam energy. The indicated error includes a 1% uncertainty in energy. The horizontal bars show the experimental resolution. The maxima in Fig. 2 at $E_{\pi\pi} = 720$ Mev indicate a resonance in the π-π interaction at approximately this energy, in rough agreement with previous measurements.[4,5]

In an effort to correlate the data with features that might be expected due to final-state interactions, we considered the following simple model.[6] It is supposed that the reaction is initiated by some vertex producing π^+ and π^-, following which a single final-state scattering always occurs. The scatterings considered are p-π^+, p-π^-, and π^+-π^-. We now assume that the amplitude for each process is the product of the initiating amplitude, C (assumed constant, independent of energy), and the free-particle scattering amplitude; furthermore we assume that the π-p scattering occurs only in the 3-3 state, and the π-π scattering in a single $J = 1$ state. Then the amplitudes for the three processes are

$$CA_{p\pi^+} = C(8\pi)^{1/2} \lambda_{p\pi^+} \exp(i\delta_{p\pi^+}) \sin\delta_{p\pi^+},$$

$$CA_{p\pi^-} = C(\tfrac{1}{3})(8\pi)^{1/2} \lambda_{p\pi^-} \exp(i\delta_{p\pi^-}) \sin\delta_{p\pi^-}$$

$$CA_{\pi\pi} = C(12\pi)^{1/2} \lambda_{\pi\pi} \exp(i\delta_{\pi\pi}) \sin\delta_{\pi\pi}$$

We neglect any considerations of proton spin and

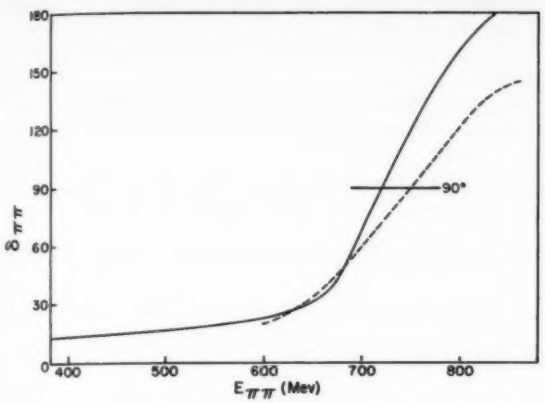

FIG. 4. $\delta_{\pi\pi}$ vs $E_{\pi\pi}$ fitting our data (solid curve), and as determined from reference 4 (dashed curve).

write the total amplitude as the sum of these amplitudes, however multiplying the π-π amplitude by an arbitrary weighting factor, η. Then we have for the production matrix element, $M^2 = C^2|A_{p\pi^+} + A_{p\pi^-} + \eta A_{\pi\pi}|^2$. For $\delta_{p\pi^+}$ and $\delta_{p\pi^-}$, we take the values from π-p scattering: $\delta(1.140) = 12°$; $\delta(1.161) = 20°$; $\delta(1.414) = 155°$.[7] Then the free parameters in the expression are $\delta_{\pi\pi}$ as a function of $E_{\pi\pi}$, C, and η. C is merely a normalizing parameter.

The solid curves in Figs. 2 and 3 are calculated from this expression with $C^2 = 0.38$ barn, $\eta = 1.6$,[8] and $\delta_{\pi\pi}(E_{\pi\pi})$ as given by the solid curve in Fig. 4. This form, which assumes a π-π resonance at $E_{\pi\pi} = 720$ Mev, of width 90 Mev,[9] reproduces the main features of the data. The dashed curves are calculated with $\delta_{\pi\pi}$ determined from the cross section given by Erwin et al.[4] (a resonance at $E_{\pi\pi} = 750$ Mev of width 150 Mev), assuming $\sigma_{\pi\pi} = 12\pi\lambda^2 \times \sin^2\delta_{\pi\pi}$. Our results indicate a resonance somewhat lower in energy and narrower in width than that of references 4 and 5. However, the lack of a reliable theory relating the resonance parameters to the measurements, and the large uncertainty in the point of highest $E_{\pi\pi}$ make our parameters for the resonance somewhat uncertain.

---

*Work supported in part by the joint program of the Office of Naval Research and the U. S. Atomic Energy Commission.

[1]S. D. Drell and F. Zachariasen, Phys. Rev. Letters 5, 66 (1960).

[2]$E_{p\pi^+}$, $E_{p\pi^-}$, $E_{\pi\pi}$, and k are related: $2m_p k = E_{p\pi^+}{}^2 + E_{p\pi^-}{}^2 + E_{\pi\pi}{}^2 - 2(m_p{}^2 + m_\pi{}^2)$. Thus in executing the program described, k must be increased as $E_{\pi\pi}$ is increased. The required change is not large, and is expected to produce only a gradual variation of the cross section; thus it should not obscure a prominent $\pi\pi$ effect. k varied from 920 to 1225 Mev as $E_{\pi\pi}$ was varied from 400 to 760 Mev.

[3]R. R. Wilson, Nuclear Instr. 1, 101 (1957).

[4]A. R. Erwin, R. March, W. D. Walker, and E. West, Phys, Phys. Rev. Letters 6, 628 (1961); also D. Stonehill, C. Baltay, H. Courant, W. Fickinger, E. C. Fowler, H. Kraybill, J. Sandweiss, J. Sanford, and H. Taft, Phys. Rev. Letters 6, 624 (1961).

[5]E. Pickup, D. K. Robinson, and E. O. Salant, Phys. Rev. Letters 7, 192 (1961).

[6]We are not aware of the existence of any treatment of final-state interactions involving three interacting particles.

[7]H. A. Bethe and F. de Hoffmann, Mesons and Fields (Row, Peterson and Company, Evanston, Illinois, 1955), Vol. 2, p. 125; W. D. Walker, J. Davis, and W. D. Shephard, Phys. Rev. 118, 1612 (1960).

[8]Unfortunately, the fit with $\eta = 1$ is not as good.

[9]This width is about equal to the experimental resolution; thus our data are consistent with a narrower width for the resonance. The calculated curves do not have the experimental resolution folded in.

MEASUREMENT OF THE LINEAR POLARIZATION OF γ RAYS BY THE ELASTIC PHOTOPRODUCTION OF π^0 ON He^4

Nicola Cabibbo

Laboratori Nazionali di Frascati del Comitato Nazionale per l'Energia Nucleare, Frascati, Italia
and Istituto di Fisica dell'Università, Roma, Italia

(Received October 27, 1961)

It is of considerable interest for the study of elementary particle physics to perform experiments with beams of linearly polarized photons.[1] These experiments require an accurate knowledge of the degree of polarization of the beam. If the beam is produced in the conventional manner, which uses the natural polarization of the bremsstrahlung perpendicular to the plane of emission, the polarization can in principle be evaluated from the geometry of the beam itself.[2]

A second method, which could produce beams of higher intensity, is based on the fact that the bremsstrahlung coherently produced on a single-crystal target can, under certain conditions, be strongly linearly polarized.[3,4] The polarization of a beam produced by this method cannot be evaluated a priori with confidence and must therefore be measured in some way.

The measurement of linear polarization requires the observation of azimuthal asymmetries in processes initiated by the rays.

The only method presently well understood is based on pair production. The difficulty here is that at high energy pair production is restricted to a narrow forward cone, and the expected asymmetries are quite small, of the order of 20-30% even for a fully polarized beam and under the best conditions.

The use of processes involving strong interacting particles is in general unsatisfactory as one then requires some information on the details of the interaction. An exception seems to be the elastic photoproduction of a neutral pion on He^4 (or in general on a spin-0 nucleus):

$$\gamma + He^4 \rightarrow \pi^0 + He^4. \tag{1}$$

This process is particularly simple as only the photon, among the particles involved, has spin different from zero. The only vector quantities here are the photon polarization vector $\vec{\epsilon}$, its momentum $\vec{k}$, and the momentum of the emitted pion, $\vec{k}'$. The amplitude for the process will therefore be proportional to the only available pseudoscalar quantity,

$$\mathfrak{M} = a[\vec{\epsilon} \cdot (\vec{k} \times \vec{k}')]. \tag{2}$$

a can depend on the photon energy and on the angle of emission of the pion. The cross section for a beam of linear polarization $\vec{P}$ is then

$$(d\sigma/d\Omega)_{\vec{P}} = [(1 - |\vec{P}|) + 2|\vec{P}|\sin^2\varphi](d\sigma/d\Omega)_{\vec{P}=0}, \tag{3}$$

where the azimuth φ is defined as the angle between the plane of emission $(\vec{k}, \vec{k}')$ and the plane of polarization $(\vec{k}, \vec{P})$.

For a fully polarized beam ($|\vec{P}| = 1$) the azimuthal distribution is simply $\sin^2\varphi$. The analyzing power of this process is therefore equal to that of a Nicol prism for visible light.

The ratio of the cross sections at 90° from $\vec{P}$ and parallel to $\vec{P}$ is

$$d\sigma_{\perp}/d\sigma_{\parallel} = (1 + |\vec{P}|)/(1 - |\vec{P}|). \tag{4}$$

This ratio is already 1.5 for a 20% polarization and increases very steeply. In this method statistics is not a problem; one should, however, be able to discriminate against such processes as

$$\gamma + He^4 \rightarrow \pi^0 + n + He^3, \tag{5}$$

$$\gamma + He^4 \rightarrow \pi^0 + \pi^0 + He^4, \text{ etc.}, \tag{6}$$

whose azimuthal distribution cannot be evaluated at present with confidence.[5]

The method proposed here has rather unique properties, especially for photons of high energy. The difficulties of the method based on pair production increase rapidly with energy, and also increasing is our ignorance of the details of other processes involving strongly interacting particles.

The author is grateful to Dr. G. Diambrini and the other members of his group for discussions which led to the present work.

[1] G. T. Hoff, Phys. Rev. 122, 665 (1961); B. De Tollis and A. Verganelakis, Phys. Rev. Letters 6, 371 (1961); M. J. Moravcsik (to be published).

[2] M. May and G. C. Wick, Phys. Rev. 81, 628 (1951); M. May, Phys. Rev. 81, 265 (1951); H. Olsen and L. C. Maximon, Phys. Rev. 114, 897 (1959); R. E. Taylor and R. F. Mozley, Phys. Rev. 117, 835 (1960); R. C. Smith and R. F. Mozley, Proceedings of the 1960 Annual International Conference on High-Energy Physics at Rochester (Interscience Publishers, Inc., New York, 1960).

[3] H. Überall, Phys. Rev. 107, 223 (1957).

[4] Experiments with a beam produced in this manner are now in progress at Frascati (G. Bologna, G. Barbiellini, G. Diambrini, G. Murtas). See also J. W.

DeWire, Laboratori Nazionali di Frascati, Nota Interna No. 87 (unpublished).

[5]Near the threshold for process (6) the relative angular momentum of the two pions will be $l=0$ (the next permitted value is $l=2$); under these conditions the azimuthal distribution of the α recoil is again uniquely determined. It is in fact $\cos^2\varphi$ for complete polarization so that contributions of (6) can mask the asymmetry in (1).

[6]For γ-ray energies below the pion threshold there exist particular photodisintegration reactions with well-defined analyzing power for the photon polarization.

PIONIC FORM FACTOR EFFECTS IN PERIPHERAL NUCLEON-NUCLEON COLLISIONS

E. Ferrari and F. Selleri
CERN, Geneva, Switzerland
(Received October 17, 1961)

There is increasing evidence that in inelastic nucleon-nucleon collisions the one-pion exchange (OPE) contribution plays an important role.[1-6] This evidence rests: (i) at a few ($\simeq$1-3) Gev on the experimental lab energy distributions[2,4] and c.m. angular distributions[3]; (ii) at many ($\gtrsim$10) Gev on the analysis of quasi-elastic scattering data,[5] of general features of the interactions[6] of emulsion experiments,[7] and of cosmic-ray interactions.[8] A further step in the analysis of such reactions consists in understanding the quantitative importance of the direct many-particle exchanges, which are expected to be increasingly important with increasing momentum transfer. The effect of these exchanges cannot, however, be revealed by comparing the OPE calculations performed till now[1,2] with experiments, because such calculations are correct only for small values of the nucleon momentum transfer.

A method for understanding the limitations of the OPE approximation has been suggested by the authors.[9] Since the matrix element for off-shell pion-nucleon scattering in the region of the 3,3 resonance has been calculated,[9] one can evaluate a peripheral graph for single (and possibly double) pion production in nucleon-nucleon collisions, by taking full account of the virtuality of the exchanged pion. This calculation is possible for energies of the πN scattering not too far from the 3,3 resonance, and is undetermined only by an unknown multiplicative function of the squared four-momentum of the virtual pion. This function is simply related to the pionic form factor of the nucleon. These facts make possible a check of the peripheral model and possibly allow the determination of the pionic form factor. If the experimental data at different energies were fitted with a unique choice of this function, then one might conclude that the OPE contribution is probably dominant also for high-momentum transfer, because the discrepancies generated from the many-particle exchanges are expected to depend also on the initial energy.

In this Letter we show that the existing experimental data do indeed suggest full dominance of the OPE term and we obtain a tentative behavior of the pionic form factor. The expression found in reference 9 for the off-shell $T=J=\frac{3}{2}$ πN scattering amplitude is[10]

$$f_{33}(u,\Delta^2)\simeq K(\Delta^2)\left(1+\frac{\Delta^2}{4m^2}\right)^{1/2}\frac{p_1}{q_1}\frac{B_0(u_\gamma,\Delta^2)}{B_0(u_\gamma,-\mu^2)}f_{33}(u,-\mu^2), \tag{1}$$

where m and μ are the nucleon and pion masses, respectively; Δ^2 is the squared four-momentum of the virtual pion; $u=(\omega-m)/m$, ω being the total c.m. energy of the πN system; $u_\gamma=0.314$ is the u value of the 3,3 resonance; $p_1=(p_{10}^2-m^2)^{1/2}$ and $q_1=(q_{10}^2-m^2)^{1/2}$ are the off-shell and on-shell c.m. momenta, where

$$p_{10}=(\omega^2+m^2+\Delta^2)/2\omega, \quad q_{10}=(\omega^2+m^2-\mu^2)/2\omega. \tag{2}$$

Finally, $K(\Delta^2)$ is the pionic form factor of the nucleon and $B_0(u,\Delta^2)$ is given by

$$B_0(u,\Delta^2)=\tfrac{4}{3}\frac{f^2}{\mu^2}\frac{u}{(u+\delta)^2}\left[1+\frac{2\delta}{u+\delta}\right], \tag{3}$$

with $f^2=0.08$ and $\delta=(\Delta^2+\mu^2)/2m^2$.

In (1) only the factor p_1/q_1 depends on both Δ^2 and u. Its u dependence is particularly strong at threshold, where it diverges like q_1^{-1}. This divergence is, however, compensated from the threshold behavior of $f_{33}(u,-\mu^2)$ which vanishes like q_1^2. Therefore, the effect of the factor p_1/q_1 on the u dependence of $f_{33}(u,\Delta^2)$ should not be too large and we put simply p_1^γ/q_1^γ in place of p_1/q_1, γ meaning "calculated at resonance."

The off-shell amplitude is then

$$f_{33}(u, \Delta^2) \simeq K(\Delta^2)\psi(\Delta^2) f_{33}(u, -\mu^2), \tag{4}$$

with

$$\psi(\Delta^2) = \frac{p_1^r}{q_1^r}\left(1 + \frac{\Delta^2}{4m^2}\right)^{1/2} \frac{u_r(u_r + 3\delta)}{(u_r + \delta)^3}. \tag{5}$$

The conclusion is thus that in the calculation of a peripheral graph the "pole approximation" discussed in reference 9 is approximately valid also for higher momentum transfers, apart from a multiplicative function of Δ^2, given by[11]

$$\phi(\Delta^2) = K^2(\Delta^2)K'(\Delta^2)\psi(\Delta^2), \tag{6}$$

K' representing the higher order corrections to the pion propagator. Assuming

$$\phi(\Delta^2) = [1 + (\Delta^2 + \mu^2)/\alpha]^{-1}, \tag{7}$$

where α is an adjustable parameter, we have tried to fit the existing experimental data[3,4,12] on the reactions

$$p + p \to p + n + \pi^+, \tag{8}$$

$$p + p \to p + p + \pi^0. \tag{9}$$

We have taken into account all the possible peripheral diagrams contributing to our reactions, according to the calculations performed in reference 2 and with the introduction of the cutoff (7) in the appropriate variable of each graph. The results for the total cross sections are shown in Table I. The comparison with the experimental data definitely shows the need for a cutoff with characteristic mass in the range 60-90 μ^2. Although the experimental total cross section seems to decrease slightly faster than the theoretical one, one sees that the discrepancy with the pole approximation can be reasonably well represented with a Δ^2-dependent function. This fact suggests an OPE contribution much more important than expected also at high Δ^2.

The differential cross sections with respect to the lab energy of the nucleons (calculated with $\alpha = 60\ \mu^2$) are shown in Figs. 1 and 2 and compared with the experimental ones. The agreement is still generally good.

If we take these results seriously we can obtain the function $K^2(\Delta^2)K'(\Delta^2)$ simply by dividing the phenomenological expression for $\phi(\Delta^2)$ by $\psi(\Delta^2)$. The behavior of the function is shown in Fig. 3 and suggests that the nucleon, as seen from a π meson, looks like a sphere of radius $\sim \mu^{-1}$ in which a much smaller core is contained. We wish to stress that this conclusion is very tentative. In fact, first the formulas used are approximate and have been applied also to regions where the 3,3 resonance is no longer dominant,[13] and secondly the existing experimental data are still rather poor. What has some chance of being not too far from reality in Fig. 3 is the steep decrease of K^2K' in the region $-\mu^2 \lesssim \Delta^2 \lesssim 10\ \mu^2$. Concerning the "core" behavior one must wait for more detailed experimental information before having any believable conclusions. The main purpose of this Letter is thus to make clear the importance of further experimental investigation of reactions (8) and (9).

The formulas for the cross sections and a more exhaustive discussion of the same problems will be contained in a forthcoming paper.

The experimental cross sections used are mainly private communications: at 0.97 Gev from Dr. D. Y. Bugg (Cambridge) and at 2.85 Gev from Dr. G. A. Smith and Professor H. Taft (Yale). We are extremely grateful to the above authors for their kindness, which made the present work possible.

Table I. Experimental and theoretical total cross sections for reactions (8) and (9) at different lab kinetic energies of the incoming proton. See references 3, 4, and 6 for the experimental data. α is the cutoff parameter defined in (7). The column $\alpha = \infty$ corresponds to calculations without cutoff.

Reaction	Energy (Gev)	Experimental cross section (mb)	Theoretical cross section (mb) $\alpha = \infty$	$\alpha = 60\mu^2$	$\alpha = 90\mu^2$
$p+p \to p+n+\pi^+$	0.97	18.4 ± 0.8	25.2	16.4	18.4
	2.00	16.06 ± 0.44	26.3	15.2	17.3
	2.85	11.45 ± 0.65	21.3	11.3	13.2
$p+p \to p+p+\pi^0$	0.97	3.8 ± 0.35	5.6	3.3	3.9
	2.85	2.9 ± 0.31	5.6	2.75	3.2

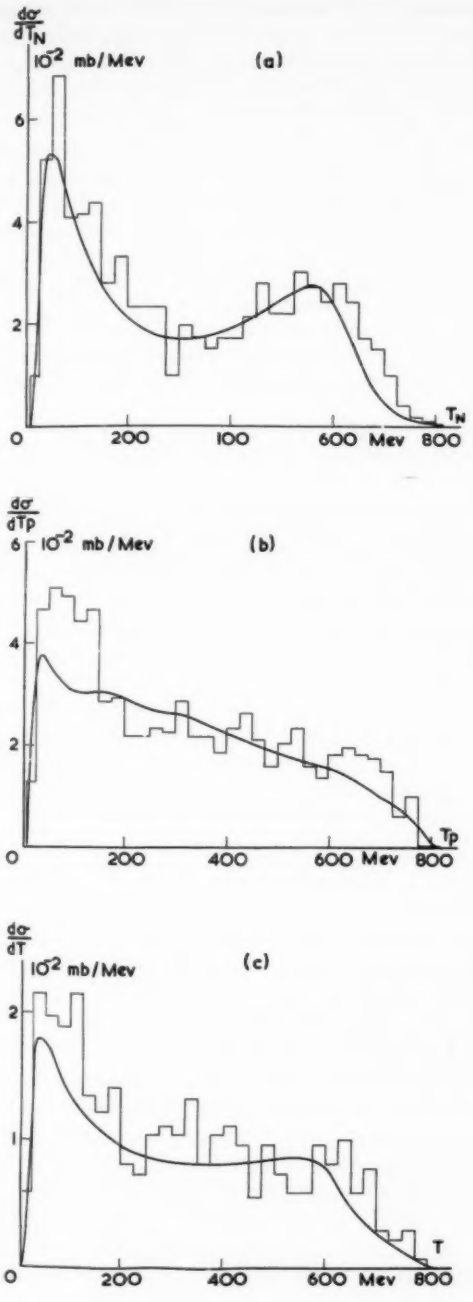

FIG. 1. Experimental (histograms) and theoretical (full lines) differential cross sections with respect to the laboratory kinetic energies at 0.97 Gev. (a) T_n: kinetic energy of the neutrons from reaction (8). (b) T_p: kinetic energy of the protons from reaction (8). (c) T: kinetic energy of the protons from reaction (9). See reference 4 for details on the experiment.

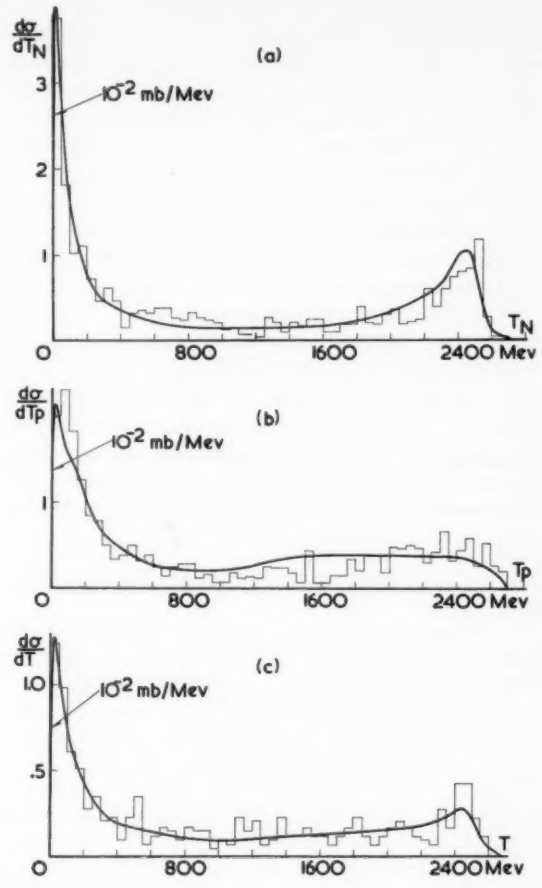

FIG. 2. Experimental (histograms) and theoretical (full lines) differential cross sections with respect to the laboratory kinetic energies at 2.85 Gev. (a) T_n: kinetic energy of the neutrons from reaction (8). (b) T_p: kinetic energy of the protons from reaction (8). (c) T: kinetic energy of the protons from reaction (9). See reference 6 for details on the experiment.

We are indebted to Dr. S. D. Drell and Professor L. Van Hove for reading the manuscript and for valuable comments.

[1]F. Selleri, Phys. Rev. Letters 6, 64 (1961).
[2]G. Da Prato, Nuovo cimento (to be published).
[3]W. J. Fickinger, E. Pickup, D. K. Robinson, and E. O. Salant, Phys. Rev. Letters 7, 196 (1961).
[4]V. Barnes, D. V. Bugg, W. P. Dodd, J. P. Kinson, and L. Riddiford, Phys. Rev. Letters 7, 285 (1961).
[5]S. D. Drell and K. Hiida, Phys. Rev. Letters 7, 199 (1961).

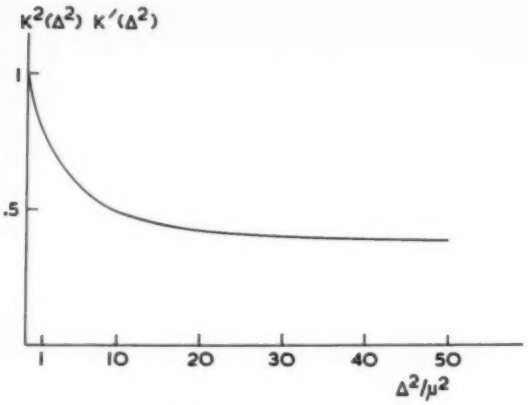

FIG. 3. The function K^2K' and its behavior with the momentum transfer, as obtained by dividing $\psi(\Delta^2)$ [see formula (5)] into $\phi(\Delta^2)$ [see formula (7)] with $\alpha = 60\mu^2$.

[6]F. Salzman and G. Salzman, Phys. Rev. 121, 1541 (1961).

[7]I. Dremin and D. S. Chernavskii, J. Exptl. Theoret. Phys. (U.S.S.R.) 38, 229 (1960) [translation: Soviet Phys.—JETP 11, 167 (1960)]; I. M. Gramenitskii, I. Dremin, V. M. Maksimenko, and D. S. Chernavskii, J. Exptl. Theoret. Phys. (U.S.S.R.) 40, 1093 (1961) [translation: Soviet Phys.—JETP 13, 771 (1961)].

[8]D. S. Chernavskii and I. Dremin, Lebedev Physical Institute, Academy of Sciences of the U.S.S.R., Moscow, Report A-29, 1960 (unpublished).

[9]E. Ferrari and F. Selleri, Nuovo cimento (to be published); see also O. Iizuka and A. Klein, Progr. Theoret. Phys. (Kyoto) 25, 1018 (1961), where the same problem is discussed.

[10]Numerical estimates prove the smallness of the term containing $\cos\delta_{33}$ in formula (66) of reference 9. We therefore neglect it here.

[11]The origin of the extra factor KK' appearing in (6) should be clear: K comes from the 3-particle vertex, where the virtual π is emitted, and K' from its propagation.

[12]G. A. Smith, H. Courant, E. C. Fowler, H. Kraybill, J. Sandweiss, and H. Taft, Phys. Rev. 123, 2160 (1961).

[13]All the performed approximations (discussed also in reference 9) could eventually be avoided. The only assumption which is essential in this analysis is the dominance of the 3,3 resonance. Its validity can be checked experimentally, for instance by comparing with the present theory the Q-value distributions of π^+p from reference 8 at fixed momentum transfer and variable initial energy.

SOLUTIONS OF THE PION-PION PARTIAL WAVE DISPERSION RELATIONS

James S. Ball and David Y. Wong
University of California at San Diego, La Jolla, California
(Received October 23, 1961)

In 1958, Chew and Mandelstam obtained a set of integral equations for the pion-pion partial wave amplitudes.[1] The underlying physical assumption of these equations is that the exchange of a pion pair in pion-pion scattering should constitute the longest range force which, in turn, dominates the scattering amplitude at low energy. Since that time, a number of authors have published various approximate solutions to these equations based on the further assumption that the major part of the two-pion force comes from the relative S and P states of the exchanged pair.[1-5] The remaining portion of the two-pion force as well as the multipion forces are usually represented by phenomenological parameters. Unfortunately, there are mathematical difficulties even in handling the P-wave exchange force which necessitates some cutoff procedure. In principle, such cutoff procedures also require adjustable parameters. It is not clear from previous results what is the minimum number of parameters required for a realistic solution of the low-energy pion-pion problem. The purpose of this Letter is to clarify this point and to present a few numerical solutions which fall within the uncertainty of the present experimental data.[6]

The coupled S- and P-wave pion-pion dispersion equations[1] are solved numerically including left-hand cuts that satisfy crossing symmetry up to a cutoff point. The remaining left-hand cut of each partial wave amplitude is replaced by a pole together with a subtraction constant at the symmetry point $\nu = -\frac{2}{3}$, where ν is the center-of-mass momentum squared in pion units. The solutions obtained are found to depend sensitively on three parameters, and no further reduction in the number of parameters seems possible if only low partial waves are kept in all absorptive amplitudes.

The S-wave subtraction constants are related by the 5 to 2 ratio:

$$\lambda \equiv -\tfrac{1}{5}A_{l=0}^{I=0}(-\tfrac{2}{3}) = -\tfrac{1}{2}A_{l=0}^{I=2}(-\tfrac{2}{3}).$$

The residue of the P-wave pole is determined by the requirement that the P-wave amplitude vanish at the threshold while the position of this pole is chosen to fit a resonance energy within the range 700-800 Mev ($5.2 < \nu_\gamma < 7.2$).[6] The residues of the S-wave poles ($I = 0, 2$) are determined by the crossing condition which relates the derivatives of the S-wave amplitudes to the value of the P-wave amplitude at the symmetry point:

$$a_1 \equiv \tfrac{3}{2} A_{l=1}^{I=1}(-\tfrac{2}{3}) = \tfrac{1}{6} A'^{I=0}_{l=0}(-\tfrac{2}{3}) = -\tfrac{1}{3} A'^{I=2}_{l=0}(-\tfrac{2}{3}).$$

The positions of the S-wave poles are left as free parameters of the problem. However, for a given set of $(\lambda, a_1, \nu_\gamma)$, the values and derivatives of all three partial wave amplitudes at the symmetry point are essentially fixed, and the higher derivatives are mainly controlled by the "near-by" left-hand cut. Hence the solution is insensitive to either the position of the S-wave poles or the cutoff point of the "near-by" left-hand discontinuity. In fact, a factor of two variation in these parameters affects the solution in the physical region by less than 5-10%. Thus our result is basically a three-parameter solution, $(\lambda, a_1, \nu_\gamma)$.

In order to fit the width of the P-wave resonance as indicated by recent experiments,[2] we choose $0.02 < a_1 \lesssim 0.05$. For a given pair of (a_1, ν_γ), λ is varied from one extreme where an $I = 0$ bound state occurs to the other extreme where the $I = 2$ ghost appears in the "near-by" left-hand region. We find that λ lies within the range ± 0.5. At present, there is no decisive experimental result on S-wave pion-pion interaction. Therefore, we only present a few typical solutions as shown in Figs. 1 and 2.

It turns out that the P-wave phenomenological pole is located quite far out on the left ($-\nu \gtrsim 10^3$) but still plays an important role in making the resonance. For the S waves, the effect of the poles in the physical region is fairly small; however, the solution does depend strongly on the subtraction constant. We therefore conclude that the "near-by left-hand cut" does not dominate even the low-energy part of the scattering in either the P or the S state. Hence the number of independent parameters cannot be reduced within the framework of keeping only low partial waves in all absorptive amplitudes.

We should mention that our solutions are qualitatively quite similar to those given by Desai,[3] who approximated the entire left-hand cut of each partial wave amplitude by a pole. Of course, our combined treatment of pology and "near-by" left-hand cuts should yield more detailed information on the structure of the amplitudes. Incidentally, we find that our solutions in general do not satisfy Desai's additional symmetry point condition involving second derivatives of the S-wave amplitudes and the first derivative of the P-wave amplitude. But we do not believe that this condition can be used to select a smaller set of solutions since the condition itself is inexact. In fact, our solutions deviate from this condition the most when the $I = 0$ contribution to the near-by left-hand cut is large. This is precisely the circumstance

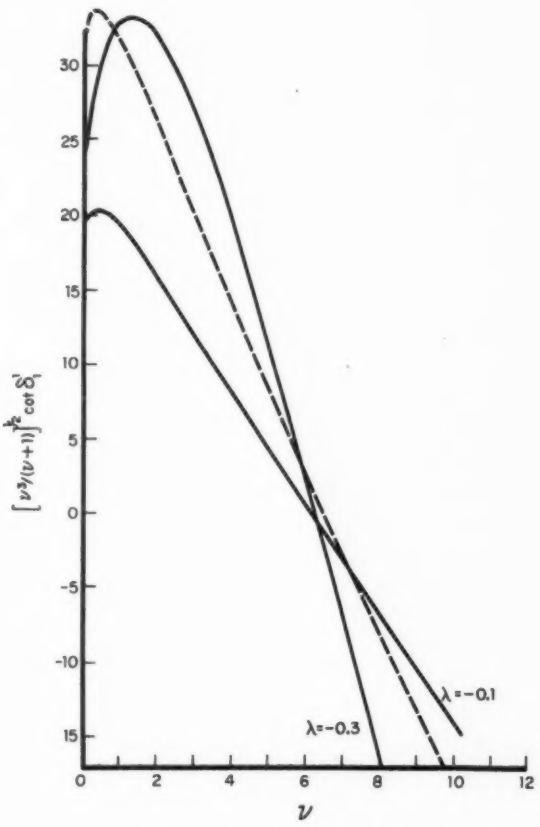

FIG. 1. A plot of $[\nu^3/(\nu+1)]^{1/2} \cot\delta_1^1$ for several solutions. The dashed curve is for $a_1 = 0.03$ and $\lambda = -0.10$. The solid curves are for $a_1 = 0.05$ with $\lambda = -0.10$ and $\lambda = -0.30$. The curvature in the neighborhood of $\nu = 0$ reflects the effect of the S wave in the crossed channel.

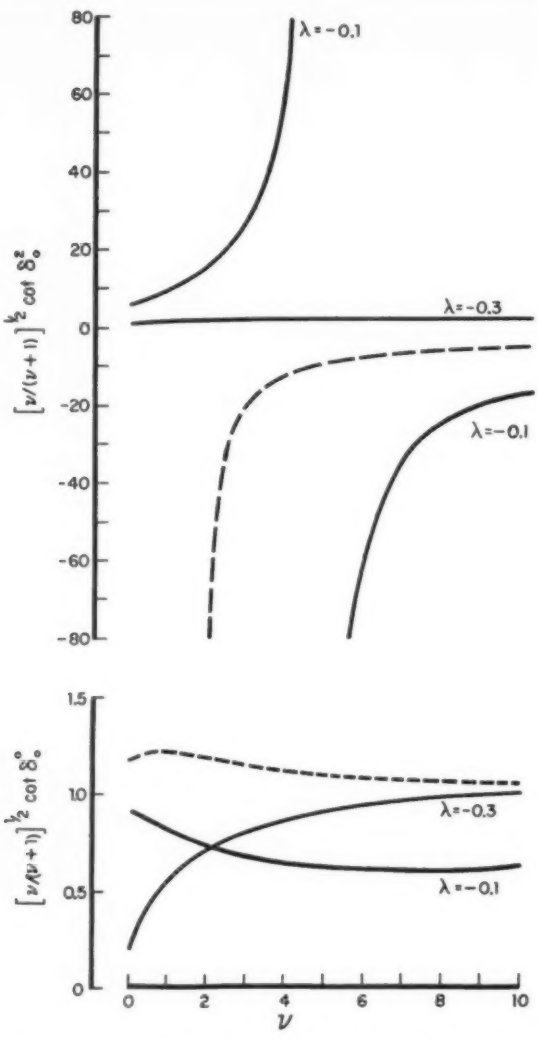

FIG. 2. A plot of $[\nu/(\nu+1)]^{1/2}\cot\delta_0^0$ and $[\nu/(\nu+1)]^{1/2}\times\cot\delta_0^2$ for various values of the parameters. The dashed curves are for $a_1=0.03$ and $\lambda=-0.10$. The solid curves are for $a_1=0.05$ with $\lambda=-0.10$ and $\lambda=-0.30$.

under which derivatives of the higher partial waves neglected in Desai's condition are not small. Since the higher derivatives are almost completely controlled by the "near-by" portion of the branch cuts, any valid symmetry point condition involving higher derivatives will automatically be satisfied by solutions which contain "near-by" cuts given by crossing symmetry.

At this point we would like to clarify some confusion on a recent paper by Bransden and Moffat.[4] In their work, it appears that the S-wave subtraction constant alone (λ) is sufficient for the determination of both the S- and P-wave amplitudes. First of all, we should point out that the left-hand discontinuity of the scattering amplitude calculated from Bransden and Moffat's solution does not agree with the left-hand cut they obtained by using crossing symmetry. This discrepancy is due to a mathematical error in their iterative procedure which leads to the wrong branch of the quadratic relation between real and imaginary parts of a function and its inverse beyond $\nu\simeq -15\,\mu^2$. In fact, the left-hand cut in their solution is practically zero for $\nu\lesssim -15\,\mu^2$, whereas the left-hand cut calculated by crossing approaches a fairly large constant (~10).[7] This explains the apparent insensitivity of their solution to the cutoff and the formal convergence of their iteration even without a cutoff. However, it is clear that the cutoff is in effect present in their solution. Now, a more important question to be asked is whether the inverse amplitude of Bransden and Moffat contains any zero on the left. The answer is that if the left-hand discontinuity is literally cut off anywhere within the range $-500\lesssim\nu<-1$, then there is a zero in the inverse function of the P-wave amplitude in the neighborhood of $\nu\sim -500$. If the scheme of Bransden and Moffat is carried out without a cutoff, then this zero will be displaced slightly from the negative real axis. In fact, this "far-away" pole in the P-wave amplitude is the major contributor to the resonance as we would expect. The position and residue of this pole are nearly independent of the left-hand cut and almost totally determined by two parameters a_1 and ξ_1 which were eventually adjusted to fit the S-wave derivative conditions at the symmetry point. It is clear that one can vary the position and width of the resonance substantially by varying a_1 and ξ_1. The derivative conditions can be satisfied by retaining a reasonable medium-range left-hand cut in each of the S-wave amplitudes. These cuts in the S-wave amplitudes are certainly no more unnatural than the far-away-yet-dominating pole in the P-wave amplitude. By allowing a variation in (a_1,ξ_1), one would end up with a three-parameter solution which would be essentially the same as ours.

In a recent paper by Zachariasen,[5] it also appears that the position and width of the P-wave resonance can be roughly determined without introducing any arbitrary parameter (aside from parameters for the S-wave amplitudes which he did not consider). Again, one can show that the far-left portion of the cut is the major contributor

to the resonance in Zachariasen's solution. Here, the left-hand cut is approximated by the Born term of a vector-meson exchange diagram divided by a D function which makes his result unitary. This D function becomes quite large in the far-left region and hence strongly suppresses the single vector-meson cut. This particular choice of the far-away left-hand cut certainly has not been justified on any theoretical basis. Thus there is ample room for doing phenomenological adjustments on the far-away left-hand cut which, we stress, could change both the position and the width of the resonance by a large amount.

So far, we have seen that "near-by" left-hand cuts do not play a very significant role in all semi-phenomenological solutions of the low-energy S-P wave pion-pion problem. This apparently contradicts the speculation that the lowest mass state provides the longest range force which dominates the low-energy scattering. However, the failure might well lie in the intuitive correspondence between near-by left-hand cuts and long-range forces.[8] It is true that partial wave expansions on the left require a cutoff, but the cutoff procedure may also cause the truncation of an important part of the long-range force which must be reinstated by phenomenological cuts or poles.

At present, it seems to us that an improved treatment of the left-hand cut may be achieved by using Regge's integral representation of the scattering amplitude instead of the conventional partial wave expansion.[9] In Regge's representation, the P-wave resonance is associated with a pole in the complex angular momentum plane. This pole produces an oscillating far-away left-hand cut as well as the usual near-by cut. As long as this pole does exist, there is no question that the oscillating cut should be included in the solution. This may well explain why far-away cuts in all phenomenological solutions seem to be quite important. Thus one may hope to reduce the number of phenomenological parameters by including the oscillating portion of the cut.

Finally, we would like to remind the reader that so far we have not taken into account inelastic scattering in the physical region. However, due to the unitarity restriction, production processes are expected to produce fairly small effects on the elastic scattering amplitude except under situations similar to those discussed by Frazer and one of us (J.S.B.).[10] The prospect of this latter type of resonances in the pion-pion system seems to be rather small.

---

[1]G. F. Chew and S. Mandelstam, Phys. Rev. 119, 467 (1960).

[2]J. G. Taylor, Phys. Rev. Letters 6, 237 (1961).

[3]B. Desai, Phys. Rev. Letters 6, 497 (1961).

[4]B. H. Bransden and J. W. Moffat, Phys. Rev. Letters 6, 708 (1961).

[5]F. Zachariasen, Phys. Rev. Letters 7, 11 (1961).

[6]J. A. Anderson, V. X. Bang, P. G. Burke, D. D. Carmony, and N. Schmitz, Phys. Rev. Letters 6, 365 (1961); D. Stonehill, C. Baltay, H. Courant, W. Fickinger, E. C. Fowler, H. Kraybill, J. Sandweiss, J. Sanford, and H. Taft, Phys. Rev. Letters 6, 624 (1960); A. R. Erwin, R. March, W. D. Walker, and E. West, Phys. Rev. Letters 6, 628 (1960); J. G. Rushbrooke and D. Radojičić, Phys. Rev. Letters 5, 567 (1960); E. Pickup, F. Ayer, and E. O. Salant, Phys. Rev. Letters 5, 161 (1960).

[7]D. Griesinger and J. Patil (private communication). We thank Dr. Griesinger and Dr. Patil for pointing out the serious discrepancy between the left-hand cut in the Bransden-Moffat solution and the left-hand cut calculated by crossing symmetry.

[8]G. F. Chew (private communication).

[9]T. Regge, Nuovo cimento 18, 947 (1960).

[10]J. S. Ball and W. R. Frazer, Phys. Rev. Letters 7, 204 (1961).

PRINCIPLE OF EQUIVALENCE FOR ALL STRONGLY INTERACTING PARTICLES WITHIN THE S-MATRIX FRAMEWORK*

Geoffrey F. Chew and S. C. Frautschi†
Lawrence Radiation Laboratory and Department of Physics, University of California, Berkeley, California
(Received October 30, 1961)

The notion, inherent in Lagrangian field theory, that certain particles are fundamental while others are complex, is becoming less and less palatable for baryons and mesons as the number of candidates for elementary status continues to increase. Sakata has proposed that only the neutron, proton, and Λ are elementary,[1] but this choice is rather arbitrary, and strong-interaction consequences of the Sakata model merely reflect the established symmetries. Heisenberg some years ago proposed an underlying spinor field that corresponds to no particular particle but which is supposed to generate all the observed particles on an equivalent basis.[2] The spirit of this approach satisfies Feynman's criterion that the correct theory should not allow a decision as to which particles are elementary,[3] but it has proved difficult to find a convincing mathematical framework in which to fit the fundamental spinor field. On the other hand, the analytically continued S matrix—with only those singularities required by unitarity[4]—has progressively, over the past half decade, appeared more and more promising as a basis for describing the strongly interacting particles. Our purpose here is to propose a formulation of the Feynman principle within the S-matrix framework.

Particles appear as energy poles of the S matrix—on the physical sheet if stable, and if unstable on an unphysical sheet. When one analyzes partial-wave elastic scattering amplitudes with neglect of competing processes, it is possible to distinguish between poles that correspond to bound states or dynamical resonances of the two-body system in question and Castillejo-Dalitz-Dyson (CDD) poles that correspond to particles "independent" of the two-body system.[5,6] However, some such CDD poles may not correspond to elementary particles when a more careful investigation includes competing channels. For example, the Dalitz-Tuan model of the Y^* describes this particle as a K-N bound state,[7] but with respect to the partial-wave elastic π-Λ amplitude such a model would normally be considered a CDD pole. Evidently one needs a criterion that emphasizes no particular configuration of particles; the criterion we propose below rests on the analytic structure of the S matrix regarded as a simultaneous function of angular momentum and energy, quantities which are meaningful for arbitrary particle combinations.

Regge has shown for elastic potential scattering[8] and Froissart for any amplitude satisfying the Mandelstam representation[9] that the S matrix can be simultaneously continued into the complex energy and angular-momentum planes. For scattering by a superposition of Yukawa potentials, all poles are associated with bound states and resonances and may be viewed either in the E plane for fixed J or in the J plane for fixed E. A corollary for the latter viewpoint is that the position, α_i, of a particular pole in the J plane is an analytic function of E, and $\alpha_i(E) = \text{constant}$ turns out not to be allowed. If at some energy the value of $\mathrm{Re}\alpha_i(E)$ passes through a positive integer or zero (with $d\,\mathrm{Re}\alpha_i/dE > 0$), one has here a physical resonance or bound state for J equal to this integer, so in general the trajectory of a single pole in the J plane as E changes corresponds to a family of "particles"—some stable and some unstable—of different J and different mass. It is possible for the trajectory of a particular pole to cross only the integer 0, but the failure to reach higher physical J values would in such a case be a dynamical circumstance and would not reflect a special role for $J = 0$. It seems intuitively clear, therefore, that any such pole appearing in the union of the complex J and E planes of the full (relativistic) S matrix cannot be associated with the usual notion of an elementary particle—which emphasizes a particular value of J. We may satisfy Feynman's principle therefore by postulating that all poles of the S matrix are of this type (Regge poles).

The reader may wonder how anything but Regge poles can occur if simultaneous continuation to complex J and E is possible. The point is that for certain internal quantum numbers, the relativistic continuation in J may be restricted to a region somewhat smaller than that for the nonrelativistic case (where the limitation in the absence of spin is $\mathrm{Re}J > -\frac{1}{2}$). In particular, the region $\mathrm{Re}J < J_{\min}(E)$, $J_{\min}(E) > 0$, might be excluded. Following arguments given by Froissart on the basis of unitarity and analyticity in linear momenta,[10] one can show that there are some E for which

$J_{\min} < 1$, but "elementary particle" energy poles, admitting no continuation in J, could be associated with the unique angular momenta $J = 0$ or $J = \frac{1}{2}$. Such a conclusion coincides with renormalizability requirements of conventional field theory, so if $J = \frac{1}{2}$ and $J = 0$ elementary particle poles actually occur in nature, it may be argued that working directly with the S matrix is simply a technique for evaluating conventional field theory.[11] On the other hand, if all baryon and meson poles admit continuation in the J plane, then conventional field theory for strong interactions is not only unnecessary but grossly misleading and perhaps even wrong.

One may regard the principle that all strongly interacting particles are associated with Regge poles as a natural extension to angular momentum of the maximal analyticity principle,[12] which heretofore has been applied only to linear momenta. Maximal analyticity in linear momenta fails to specify precisely the asymptotic behavior in momentum transfer, which is the controlling factor in determining the region of analyticity in the J plane.[9]

How is one to distinguish experimentally between Regge poles and elementary particle poles? An essential characteristic of a Regge pole is that it moves in the J plane as a function of E, the trajectory being the same—regardless of multiplicity—for all S-matrix elements having the internal quantum numbers of the pole.[13] Experiments to establish this trajectory will be of two types, depending on the value of $s = E^2$. For $s > 0$ one will seek to identify the existence of families of particles. Blankenbecler and Goldberger, for example, have mentioned the possibility that the nucleon is only the $J = \frac{1}{2}$ member of a family that may have unstable higher J members ($J = \frac{5}{2}$, $\frac{9}{2}$, etc.) to be found among the resonances of multiparticle systems with the same baryon number, isotopic spin, etc., as the nucleon.[14] One will seek to show that the angular momentum of such particles is a monotonic function of their masses, but since only discrete J values can be observed and the total number of family members is not necessarily large (there may be only one physical value crossed by the trajectory) one may confidently anticipate situations where the Regge character of a pole is not convincingly established by experiments with $s > 0$.

For $s < 0$, on the other hand, if the qualitative arguments about "strips" in the Mandelstam diagram presented by the authors can be taken seriously,[15] then one should be able to study the trajectory $\alpha_i(s)$ in a continuous sense within the strip $s_{\min}{}^i < s < 0$, where $s_{\min}{}^i$ is defined by $\alpha_i(s_{\min}{}^i) = J_{\min}(s_{\min}{}^i)$. Here one is working experimentally in a "crossed" reaction where s is the negative square of a momentum transfer. It may turn out for some poles that $s_{\min}{}^i$ is greater than zero and the strip in question does not exist, but the essence of our earlier argument is that there should be important situations where the trajectory of the Regge pole is still inside the region of analyticity $\mathrm{Re}J > J_{\min}$ for a range of negative s. Consider, for instance, the possibility that the recently discovered ρ meson is associated with a Regge pole whose internal quantum numbers are those of an $I = 1$ two-pion configuration.[16] Then we know experimentally one point on the curve $\mathrm{Re}\alpha_\rho(s)$, namely, $\mathrm{Re}\alpha_\rho(28\, m_\pi{}^2) = 1$, since the spin of the ρ meson is 1 and its mass $5.3\, m_\pi$. By analogy with potential theory, $d\,\mathrm{Re}\alpha_\rho/ds$ is probably positive for energies below this resonance.[8] However, it seems likely for these quantum numbers that we have $J_{\min} \leq 0$,[16] so there is a chance that at zero or even slightly negative s, the value of α_ρ still is larger than $J_{\min}$. [$\alpha(s)$ is real for real s below the lowest two-particle threshold, which here occurs at $s = 4m_\pi{}^2$.] In such a circumstance the Regge pole should dominate the high-energy behavior of the crossed channel near the forward (or backward) direction where $|s|$ is small. In particular, in a two-body reaction, such as neutron-proton exchange scattering with center-of-mass energy $t^{1/2}$, the amplitude will have an energy dependence $\propto t^{\alpha(s)}$. Thus it may be possible, by studying the asymptotic energy variation of the backward peak in n-p scattering, to trace out a portion of the trajectory of the Regge pole associated with the ρ meson.[17]

In general, when forward or backward high-energy scattering is controlled by a Regge pole, one finds by an elementary calculation that

$$d\sigma/d\Delta^2 \sim F(\Delta^2)E^{2[\alpha(\Delta^2)-1]}, \qquad (1)$$

where $\Delta = (-s)^{1/2}$ is the momentum transfer, and the lab energy E is proportional to t. Now α is expected to be a monotonically decreasing function of Δ^2, so two characteristic predictions are made: (a) The width of the peak should decrease logarithmically as E increases. (b) The tail of the peak should fall off exponentially with Δ^2 [the function $F(\Delta^2)$, which is related to the residue of the Regge pole, is expected to be an analytic function of Δ^2]. Both these effects are seen more clearly in a linear approximation for $\alpha(s)$:

$$\alpha(s) \approx \alpha(0) + s\alpha'(0), \qquad (2)$$

from which follows

$$d\sigma/d\Delta^2 \sim F(\Delta^2)E^{-2[1-\alpha(0)]}\exp\{-[2\alpha'(0)\ln E]\Delta^2\}. \quad (3)$$

A third important prediction is that the same constants, $\alpha(0)$, $\alpha'(0)$, etc., should control all forward or backward peaks that relate to the same set of quantum numbers. Thus the trajectory of α_ρ, for example, should control backward $\pi^+\pi^0$ and K^+K^0 scattering if it controls backward np scattering.

In contrast to the above, an elementary particle of spin S would give a forward or backward peak characterized by replacing $\alpha(\Delta^2)$ by S, a constant, in formula (1). Thus the magnitude should fall off less rapidly and the shape of the peak should not change with increasing energy; also the tail should not be exponential. Of course, we already know from its quantum numbers that the ρ meson cannot be an elementary particle in the conventional sense, and that it almost certainly is associated with a Regge pole. The interesting cases will be those where the spin is equal to 0 or $\frac{1}{2}$. Here the effect on backward peaks of crossed reactions may be difficult to find experimentally (because J is smaller) but a detailed theoretical analysis of the various possibilities seems well worthwhile.[18] For example, it appears that to test whether the neutron is elementary one need only determine whether in backward π^+p scattering $d\sigma/d\Delta^2$ decreases like $1/E$ at high energy, or at a faster rate corresponding to a Regge pole with $\alpha(0)<\frac{1}{2}$.

It is a fascinating possibility that all forward (diffraction) peaks may be controlled by a Regge pole having the same internal quantum numbers as the vacuum and with a trajectory such that $\alpha_{\text{vac}}(s=0)=1$. Constant high-energy total cross sections satisfying the Pomeranchuk conditions are then guaranteed. Because of the even parity of the vacuum, odd J values here have no physical significance, but if at some positive energy $\text{Re}\alpha_{\text{vac}}$ crosses the value 2, there would be a spin-two particle associated with this pole. We apparently must exclude $J=0$ from the region of analyticity if the trajectory of this Regge pole is "normal," because then we would expect $\alpha_{\text{vac}}(s)$ to vanish at a negative value of s, corresponding to a ghost $J=0$ particle. An exceptional status for the quantum numbers of the vacuum appears unavoidable whether or not diffraction scattering is related to a Regge pole. The existence of constant high-energy cross sections will inevitably put special requirements on analyticity properties in J for these particular quantum numbers. Our principle of maximal analyticity in J, therefore, must be amended with the phrase, "consistent with the principle of maximum strength for strong interactions."[15]

The association of high-energy forward and backward peaks with Regge poles, together with the principle of maximal analyticity in J, provides a natural explanation of why low-mass particles tend to have low internal quantum numbers (isotopic spin, strangeness, and baryon number). High-energy peaks evidently are a result of coherence in scattering. Maximum coherence—i.e., the maximum value of $\alpha(0)$—occurs for exchange of the quantum numbers of the vacuum; the degree of coherence progressively decreases with an increase in the quantum numbers of the exchanged system—with a consequent decrease in the value of $\alpha(0)$. (This effect is explicitly illustrated for $\pi\pi$ scattering in reference 16.) By analytic continuation, such a correlation between $\alpha(0)$ and internal quantum numbers is likely to be maintained for $\alpha(s)$ in the region of positive s, with the consequence that low-energy bound states and resonances are most likely to occur for low isotopic spin, low strangeness, and low baryon number.

We note, in conclusion, two experimentally attractive features of the Regge-pole hypothesis for diffraction peaks: (a) Gribov's argument that total cross sections must decrease is circumvented.[19] He assumed a factorable high-energy dependence on Δ^2 and E, which is not true for formula (1). (b) As noted by Lovelace,[20] the observed exponential behavior in Δ^2 of the diffraction "tail" is difficult to understand on a classical basis but, as we have seen above, it follows immediately from a Regge pole. The disagreeable feature is the predicted logarithmic decrease of the elastic cross section while the total cross section remains constant. However, if one admits that, after all, this may not be a classical situation, no clear argument can be made that such behavior is inadmissible. We must wait for experiment to decide. A related experimental test that may be immediately possible is to see if the exponential occurring in the tail of pp diffraction scattering is the same as that occurring in πp and Kp scattering.

We should like to acknowledge enormous benefit received from conversations with M. Froissart, M. Gell-Mann, and S. Mandelstam, without implying that they agree with all the arguments given here.

*This work was supported by the U. S. Atomic Energy Commission.

†Present address: Department of Physics, Cornell University, Ithaca, New York.

[1]S. Sakata, Progr. Theoret. Phys. (Kyoto) 16, 686 (1956).

[2]W. Heisenberg, Revs. Modern Phys. 29, 269 (1957).

[3]R. Feynman (private communication).

[4]A review of the S-matrix theory of strong interactions has recently been given by one of the authors (G.F.C.) in a report at the La Jolla Conference on the Theory of Weak and Strong Interactions [Lawrence Radiation Laboratory Report UCRL-9701, 1961 (unpublished)]. Two more detailed surveys are in press: G. F. Chew, The S-Matrix Theory of Strong Interactions (W. A. Benjamin and Company, New York, 1961); and S. Mandelstam, in Reports on Progress in Physics [The Physical Society, London (to be published)].

[5]L. Castillejo, R. Dalitz, and F. Dyson, Phys. Rev. 101, 453 (1956).

[6]A recent discussion of poles in elastic amplitudes has been given by the authors, Phys. Rev. 124, 264 (1961). See also the reviews of reference 4.

[7]R. H. Dalitz and S. F. Tuan, Ann. Phys. 3, 307 (1960).

[8]T. Regge, Nuovo cimento 14, 951 (1959); 18, 947 (1960).

[9]M. Froissart (Princeton University), Report to the La Jolla Conference on the Theory of Weak and Strong Interactions, La Jolla, 1961 (unpublished).

[10]M. Froissart, Phys. Rev. 123, 1053 (1961).

[11]S. Mandelstam, Report to the 1961 Solvay Conference on Field Theory, Brussels, 1961 (to be published); see also the last two reviews listed in reference 4.

[12]G. F. Chew, in Dispersion Relations, edited by G. R. Screaton (Oliver and Boyd, Ltd., Edinburgh, 1960), p. 167; and the reviews listed in reference 4. Also see H. P. Stapp, Lawrence Radiation Laboratory Report UCRL-9804, 1961 (unpublished).

[13]Unitarity couples all S-matrix elements of the same quantum numbers, so that a pole in one must appear in all. The possibility of continuation in the J plane has so far been demonstrated only for two-body elements, but we assume for the discussion here that it has a meaning in general. Note that a particular Regge pole is characterized among other things by its parity, so that only alternate J values have a physical meaning. This somewhat confusing point is discussed in reference 14 and will be elaborated in a forthcoming paper by M. Gell-Mann, S. C. Frautschi, and F. Zachariasen.

[14]R. Blankenbecler and M. L. Goldberger (to be published).

[15]G. F. Chew and S. C. Frautschi, Phys. Rev. 123, 1478 (1961).

[16]This possibility is discussed in detail in a forthcoming paper by G. F. Chew, S. C. Frautschi, and S. Mandelstam, Lawrence Radiation Laboratory Report UCRL-9925 (unpublished).

[17]One might expect the pole associated with the pion, whether Regge-like or elementary, to contribute to the backward n-p peak. Since the spin of the pion is zero, however, such a pole would probably lead to a lower power of t than that associated with the ρ. The ω has spin one, but because its isotopic spin is zero, it will not appear in backward n-p scattering.

[18]Such an analysis is being carried out by S. Frautschi, M. Gell-Mann, and F. Zachariasen.

[19]V. N. Gribov, Nuclear Phys. 22, 249 (1961).

[20]C. Lovelace (to be published).

CONTENTS

Physical Review Letters Volume 7, No. 10 November 15, 1961

Specific Heat of Solid He^3 . . . . . E. C. Heltemes and C. A. Swenson 363
Magnetic Properties of He^3 at Pressures Near the Minimum in the Melting Curve . . . . . A. C. Anderson, W. Reese, and J. C. Wheatley 366
Behavior of Strongly Shocked Carbon . . . . . B. J. Alder and R. H. Christian 367
Magnetoresistance of Transition Metals in the High-Field Limit . . . . . E. Fawcett 370
Experimental Evidence of Birefringence by Free Carriers in Semiconductors . . . . . K. J. Schmidt-Tiedemann 372
Interpretation of the Electromagnetic Radiation from Electron Passage Through Metal Films . . . . . V. P. Silin and E. P. Fetisov 374
$K^+ + d$ Charge-Exchange Reaction from 52 to 456 Mev . . . . . William Slater, Donald H. Stork, Harold K. Ticho, Wonyong Lee, William Chinowsky, Gerson Goldhaber, Sulamith Goldhaber, and Thomas O'Halloran 376
Evidence for a Pion-Pion Resonance from Photoproduction of Pion Pairs . . . . . D. McLeod, S. Richert, and A. Silverman 383
Measurement of the Linear Polarization of γ Rays by the Elastic Photoproduction of π^0 on He^4 . . . . . Nicola Cabibbo 386
Pionic Form Factor Effects in Peripheral Nucleon-Nucleon Collisions . . . . . E. Ferrari and F. Selleri 387
Solutions of the Pion-Pion Partial Wave Dispersion Relations . . James S. Ball and David Y. Wong 390
Principle of Equivalence for All Strongly Interacting Particles within the S-Matrix Framework . . . . . Geoffrey F. Chew and S. C. Frautschi 394
ABSTRACTS of Articles to be published in The Physical Review . . . . . Separate Section

LITHO IN USA
PALMER & OLIVER

, 1961

n 363
.
y 366
n 367
tt 370
.
n 372
.
v 374
,
,
n 378
.
n 383
.
o 386
.
ri 387
g 390
.
hi 394
Section

LITHO IN USA
MER & OLIVE